MEASUREMENT AND PREDICTION OF GAS HYDRATE EQUILIBRIUM CONDITIONS IN THE PRESENCE OF INHIBITORS

By

HUIJIE WU

B.Sc., Inner Mongolia Polytechnic University, 1994

A THESIS SUBMITTED IN PARTIAL FULFILLMENT
OF THE REQUIREMENTS FOR THE DEGREE OF

MASTER OF APPLIED SCIENCE

in

THE FACULTY OF GRADUATE STUDIES

(CHEMICAL AND BIOLOGICAL ENGINEERING)

THE UNIVERSITY OF BRITISH COLUMBIA

October 2005

ABSTRACT

Gas hydrates are crystals which are formed by water and small gas molecules at low temperature and high pressure. Hydrate for many years have been a problem in oil and gas industries because hydrate formation may plug the pipelines or valves and might also cause blowout in the drilling operations. In order to avoid hydrate formation, inhibitors are introduced to increase the pressure needed at a given temperature for hydrates formation. Generally used inhibitors in oil and gas industries are methanol, glycerol, ethylence glycol and triethylene glycol.

Knowledge of the equilibrium hydrate-forming conditions is necessary for the rational and economic design of processes in the chemical, oil, gas, and other industries where hydrate formation is encountered. It is important to measure the incipient hydrate formation conditions for the systems containing different inhibitors, and also it is important to have available reliable methods for calculating the impact of the addition of these chemicals into the aqueous phase on the equilibrium hydrate formation conditions (inhibiting effect).

In this work, the inhibiting effects of triethylene glycol (TEG) and glycerol in methane-ethane and methane-propane gas mixture hydrate formation systems were measured. The data showed that TEG (20.0wt% and 30.0wt %) and glycerol (20.0wt %) have considerable inhibiting effect on hydrate formation.

These data are also valuable for validating the hydrate prediction models. Several models have been published based on cubic equations of state. In this work the Trebble-Bishnoi equation was used. The results were found to be in very good agreement with the data. The statistical associating fluid theory (SAFT) equation of state was also employed for the prediction of the thermodynamic inhibiting effect of methanol, glycerol, ethylene glycol and triethylene glycol on single gas hydrate formation. The results were found to be in satisfactory to excellent agreement with the experimental data. The SAFT equation takes into account hard sphere repulsion, hard chain formation, dispersion and association. This enables this model to be able to correlate and predict successfully systems containing water, alcohols and hydrocarbons.

TABLE OF CONTENTS

LIST OF TABLES

LIST OF FIGURES

LIST OF SYMBOLS

A = Helmholtz free energy, J

C = Langmuir constant, 1/MPa

Cp = heat capacity, J/mol K

d = hard-sphere diameter, 1×10^{-10} m

f = fugacity, MPa

g. = radius distribution function

k = Boltzmann constant, J K^{-1}

K = Boltzman's constant, J/K

m = effective number of segments

M = number of associate sites

n = number of components

nc = number of hydrate forming substances

N = number of molecules

N_A = Avogadro constant, 6.02217×10^{23} mol^{-1}

r = radial distance from center of hydrate cavity, m

R = gas constant, 8.3143 J mol^{-1} K^{-1}

R_m = type m spherical cavity radius, m

P = pressure, MPa

T = absolute temperature, K

v= molar volume, m^3/mole

$W(r)$ = cell potential function, J

x = mole fraction in liquid phase

x_i = mole fraction of component i

X_i^A = mole fraction of molecule i not bonded at site A

y = mole fraction in vapor phase

Z = compressibility factor

Greek letters

$\beta = 1/kT$

ε/k = energy parameter of dispersion, K

ε^{AB}/k = energy parameter of association between sites A and B, K

κ^{AB} = bonding volume

Δ^{AB} = association strength between sites A and B

μ = chemical potential

ρ = molar density, mol/m^{-3}

ρ_n = number density, m^{-3}

σ = soft-sphere diameter,. 1×10^{-10} m

v_m = number of cavities of type m

Subscripts

i, j, k = components

m = type of cavity

w = water

Superscripts

assoc = association interaction

A, B = association site

chain = hard-sphere chain

disp = dispersion interaction

hs = hard-sphere

res = residual term

H = hydrate

L = liquid

L^o = pure liquid water

MT = empty lattice

o = reference conditions of 273.15 K and zero absolute pressure

V = vapor

ACKNOWLEDGEMENTS

I extend my sincere gratitude to my supervisor **Dr. Peter Englezos**, for giving me this research opportunity and for providing me with invaluable guidance, excellent suggestions, encouragement, care and attention throughout the study.

I am very grateful to my husband Dr. Xiaosen Li for his great support and help.

I would also like to thank my research group Dr. Ju Dong Lee, Robin, Rajnish, Shivamurthy and Praveen for their invaluable discussions, help and suggestions. I would like to thank the excellent staff members of Chemical Engineering department for providing necessary help whenever required.

My deepest love and gratitude is felt for my parents and family members for their never ending encouragement and support. This would have been impossible without them. Last but not the least, I would like to thank all my friends who are directly or indirectly involved in making this dream come true.

1. Introduction

Gas hydrates are nonstoichometric crystalline inclusion compounds. At a low temperature and high pressure, water molecules linked together through hydrogen bonding create a lattice-like structure with cavities (host lattice) that can enclose a large variety of molecules (guests). The interaction between the water molecules and the guests molecules are just Van der Waals forces. Molecules which do not interfere with the hydrogen bonding of water molecules and have a diameter that is smaller than the diameter of the cavity can render the structure stable under suitable pressure and temperature conditions (Davidson, 1973; Sloan, 1990).Typical hydrate-forming substances include CH_4, C_2H_6, C_3H_8, CO_2, and H_2S. Naturally occurring clathrate hydrates in the earth contain mostly methane and which are regarded as a future energy resource (Englezos, 1993).

Sir Humphry Davy was the first person to report clathrate hydrate formation in 1810. This was chlorine hydrate and this was confirmed by Farady in 1823. Gas hydrates crystallize in three different structures: cubic structure I (sI), cubic structure II (sII), or hexagonal structure H (sH) (Ripmeester et al. 1987; Ripmeester and Ratcliffe, 1990; Ripmeester et al. 1994). The basic cavity formed by hydrogen-bonded water molecules is the pentagonal dodecahedron (5^{12}). A unit cell of gas hydrate structure I is shown in figure 1

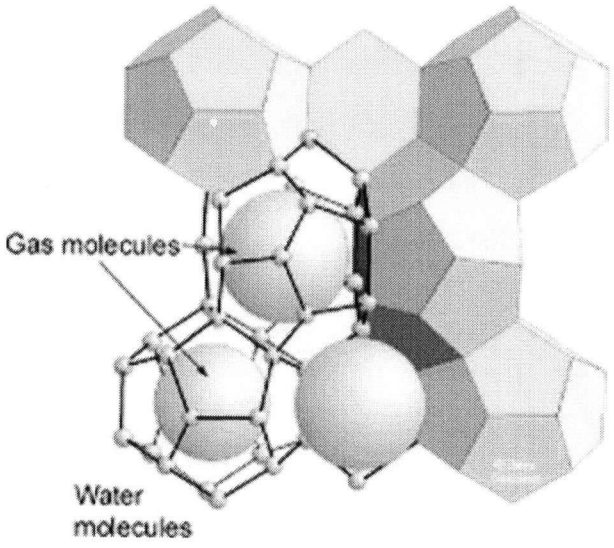

Figure 1: Diagram of gas hydrate structure I.

Vast quantities of naturally occurring gas hydrates, containing mostly methane, were discovered in the earth's crust (Katz, 1971; Makogon et al. 1972). Kvenvolden (1988) estimated that 10^{16} m^3 of methane gas exist in hydrate. The hydrates are distributed in the deep oceans and permafrost regions. One volume of hydrate contains as much as 164 volumes of gas at standard temperature and pressure condition (STP). Thus the amount of methane in hydrate state exceeds the total combined fossil fuel and it is a great potential energy resource for the future.

Hydrates also generally are a serious problem in the gas and oil industry. Hydrate formation may plug the pipelines or valves and also erode equipment surfaces (Sloan, 1998). Viscosity of crude oil may change due to the formation of hydrates. At drilling sites, dissociation of solid hydrates present in natural formations may cause damage and leakage due to uncontrolled gas release, blowouts of the wellhead, etc. The released methane contributes to greenhouse effect. Because of these devastating and often costly consequences of hydrate formation, methods of slowing hydrate solids development in gas and oil streams have been an attractive research project for a number of years.

Hydrate formation can be prevented by using any of the following methods.

- Adjusting the temperature and pressure until hydrate formation is not favored.
- Dehydrating a gas stream to prevent a free water phase.
- Inhibiting hydrate formation by the addition of chemicals in the water phase.

Hydrate inhibition is typically employed when it is not cost effective to install a full dehydration unit, or when an operating dehydration unit cannot obtain the desired dew point depressions. Inhibition utilizes the injection of a known hydrate inhibitor into the process upstream of the location where solids formation is predicted to occur. Thermodynamic inhibitors prevent hydrate formation by shifting the equilibrium conditions so that lower temperatures and higher pressures are required to form hydrates. The hydrate suppression ability of the inhibitors is a consequence of their ability to reduce the activity of water. Commonly used thermodynamic inhibitors are methanol, ethylene glycol (EG), glycerol and triethylene glycol (TEG).

To avoid the problems associated with hydrate formation, to exploit the hydrates as an energy resource or to utilize hydrates to develop new technologies, there is a need to obtain phase equilibrium data and develop prediction methods for pure water as well as for aqueous systems containing inhibitors.

The studies on clathrate hydrate equilibrium focus on gathering incipient equilibrium hydrate formation data and on developing predictive methods for the calculation of phase equilibria. The incipient formation conditions refer to the situation in which an infinitesimal amount of the hydrate phase is present in equilibrium with fluid phases. Knowledge of the equilibrium hydrate-forming conditions is necessary for the rational and economic design of processes in the chemical, oil, and other industries where hydrate formation is encountered. (Englezos, 1993).

The thermodynamics of hydrate formation has been studied extensively over the years and data for several thermodynamic inhibitors have been obtained. However, the data for some specific inhibitors, such as triethylene glycol, are not adequate. Such data are useful in industrial design applications as well as for testing predictive models.

Several methods have been published which predict hydrate formation in the presence of inhibitors and especially methanol. The methods are usually based on using cubic equations of state for the fluid phases.

Statistical associated fluid theory (SAFT) has been investigated extensively since proposed, and is very advantageous over traditional cubic equations of state. The theory is quite appropriate for associating fluids. Hence, it is suitable for alcohol-water systems.

This work will try to obtain more incipient equilibrium hydrate formation data for the systems containing the inhibitor of triethylene glycol and glycerol to detect their inhibiting abilities and then make predictions using the Trebble-Bishnoi and SAFT equations of state.

2. Literature Review and Research Objectives

2.1 Structure of gas hydrate

Clathrates are solid solutions of a volatile solute in a host lattice (van der Waals, 1956). The solvent is known as the empty hydrate lattice formed by water molecules that are linked together with hydrogen bonds and form a three-dimensional structure with cavities. Gas molecules, which do not interfere with the hydrogen bonding of water molecules and have a diameter that is smaller than the diameter of the cavity, can be enclosed in the lattices.

In a hydrate, the species forming the lattice is commonly called the host, while the caged component is called the guest. The host-lattice is thermodynamically unstable without the presence of a guest molecule in the cavity. The guest molecule, which stabilizes the lattice, is held in place inside the lattice by weak van der Waals forces.

There are three known gas hydrate structures: Structure I; Structure II; Structure H (Ripmesster et al. 1987). Structure I consists of two different types of cavities. The first cavity is called a pentagonal dodecahedron (5^{12}) which is present in all the gas hydrate structures. Second type of cavity is called tetrakaidecahedron ($5^{12}6^2$), which is larger than the dodecahedron. A unit cell of this structure consists of six large $5^{12}6^2$ cavities, and two small 5^{12} cavities created by 46 water molecules. Common structure I forming gases are methane, ethane and carbon dioxide. Structure II hydrate consists of 16 small (5^{12}) and 8 large cavities ($5^{12}6^4$) made up by 136 water molecules. Structure H has the basic 5^{12} cage and the two other cavities consist of a $4^3 5^6 6^3$ cage and a $5^{12}6^8$. Table 1.is the Structural properties of hydrates (Sloan, 1998)

Table 1. Structural properties of hydrates (Sloan, 1998)

	Structure I	Structure II	Structure H
Cavity types	5^{12}, $5^{12}6^2$	5^{12}, $5^{12}6^4$	5^{12}, $4^3 5^6 6^3$, $5^{12}6^8$
Cages/unit cell	2, 6	16, 8	3, 2, 1
Crystal type	Cubic	Cubic	Hexagonal

2.2. Thermodynamic experimental studies

One of the traditional methods for preventing the hydrate formation is to use inhibiting substances (methanol, glycols and glycerol) during the industrial operation. Electrolytes are also known to be strong thermodynamic inhibitors. Measurement of the effect of the inhibitors on the incipient equilibrium gas hydrate formation conditions is necessary for process design. For example, these thermodynamic data can be used directly in the design of operations in the oil and gas industry involving the search, recovery, transport, or processing of hydrocarbon fluids. Moreover, the thermodynamic data are needed to test hydrate formation prediction methods.

Experimental data regarding the effect of thermodynamic inhibitors continue to appear in the literature. Song and Kobayashi (1989) measured the inhibiting effect of methanol and ethylene glycol on the incipient hydrate formation conditions from a mixture of methane and propane. Dholabhai et al. (1991a) and Englezos and Bishnoi (1991) presented experimental data on methane and ethane hydrate formation in aqueous mixed electrolyte solutions. Svartas and Fadnes (1992) presented data on the inhibition of methanol. It was found that methanol doesn't promote hydrate formation at concentrations for which Makogon (1981) and Berecz and Balla-Achs (1983) reported the opposite effect. Englezos and Ngan (1993a) measured incipient hydrate formation conditions for propane in aqueous mixed electrolyte solutions. Englezos and Ngan (1994) also measured incipient phase equilibrium data for methane, ethane and propane hydrate formation in aqueous solutions of polyethylene oxide (PEO). The results indicate a very weak inhibiting effect compared with the effect of electrolytes and alcohols on the equilibrium hydrate formation conditions. Experimental data for CO_2 hydrates in aqueous solutions containing methanol and electrolytes were reported by Dholabhai at al. (1996). Breland and Englezos (1996) provided equilibrium condition data for carbon dioxide hydrate in pure water and aqueous glycerol solutions in order to evaluate the effectiveness of glycerol as an inhibiting agent. It was shown that glycerol has a considerable inhibiting effect on carbon dioxide hydrate formation though it was not as effective as an inhibiting agent as sodium chloride or methanol. Bishnoi et al. (1999) measured equilibrium conditions for hydrate formation frrom a ternary mixture of methane, propane and carbon dioxide, and from a natural gas mixture in the presence of electrolytes and methanol. Experimental three phase equilibrium data for two mixtures of methane and CO_2 in the presence of methanol, ethylene glycol and electrolytes were obtained by

Dholabhai et al. (1997). Servio et al. (1999) measured incipient equilibrium gas hydrates formation conditions for the CO_2-CH_4-neohexane-NaCl-H_2O and CH_4-polypropylene glycol-NaCl-H_2O systems. Mahmodaghdam and Bishnoi.(2002) obtained equilibrium experimental data for methane, ethane, and propane incipient hydrae formation in the presence of diethylene glycol and that for propane in the presence in the presence of ethylene glycol were obtained. Roch (2003) measured 3-phase hydrate equilibrium of methane-rich gas mixtures in pure water and in the presence of different salts, methanol and glycol were investigated. Eichholz et al. (2004) provided experimental three-phase hydrate equilibrium data for methane hydrates in aqueous solutions of ethylene glycol and sodium chloride.

Triethylene glycol (TEG) and glycerol are industrially used chemicals to inhibit the formation of gas hydrates. Ross and Toczylkin (1992) have presented data on the effect of TEG on methane and ethane gas hydrate. Servio and Englezos (1997) measured incipient equilibrium propane hydrates formation conditions in aqueous triethylene glycol solution. TEG was shown to have considerable inhibiting effect on propane hydrate formation. Breland and Englezos measured the equilibrium hydrate formation data for carbon dioxide in aqueous glycerol solutions. It was shown that inhibiting effectiveness of TEG is comparable to glycerol at the same weight % basis, but they are weaker than methanol. In order to obtain further knowledge about the inhibition ability of the TEG and glycerol and provide data for developing and testing the predictive methods for hydrate equilibrium, more experiment data is required.

2.3. Thermodynamic models

Several models have been proposed over the years to predict the equilibrium hydrate formation conditions. Hammerschmidt (1934) developed the first method used in the industry for predicting the inhibiting effect of methanol. The method is empirical and the reliability of the calculations is variable (Ng, 1985). Anderson and Prausnitz (1986) presented a thermodynamics-based method for calculating the inhibiting effects of methanol. They used van der Waals-Platteuw model for the solid hydrate phase, Redich-Kwong equation of state for the vapour phase and the UNIQUAC model for the liquid phase. Henry's constants were used for calculating the fugacities of components in their supercritical state in the liquid phase. Furthermore, empirical correlations were used for calculating the molar volumes, partial molar

volumes at infinite dilution and the fugacity of hypothetical liquid water below the ice-point temperature. Robinson and Ng (1986) have mentioned a commercial computer program which allows the calculation of the depression of hydrate formation temperatures due to methanol. A thermodynamics-based computation methodology was presented by Englezos et al. (1991) for calculating the depression effects of methanol and the amounts of methanol required, which used the Trebble-Bishnoi equation of state for the liquid and vapor phases and the van der Waals-Platteeuw model for the solid hydrate phase. Avlonitis et al. (1991) employed one of the established three-parameter cubic equations of state (EOS) for all fluid phases and developed special mixing rules for asymmetric interactions. However, it should be noted that the traditional models such as cubic equations are not suitable models for associating fluids such as glycols which is associating fluids.

The statistical associating fluid theory (SAFT) is based on Wertheim's first-order thermodynamic perturbation theory (Wertheim, 1986) for associating fluids, and has been developed very rapidly in recent years (Muller and Gubbins, 2001). Molecular-based equations of states with salient physical meaningful parameters are generally more reliable than empirical models for extrapolation and prediction. Consequently, SAFT has been used to model successfully a wide variety of the thermodynamic properties and phase equilibria for industrially important fluids containing n-alkane mixtures and alcohols aqueous solutions (Muller and Gubbins, 2001; Voutsas et al. 2000; Pfohl et al. 1999). Recently we successfully used the SAFT equation to model the phase equilibria of the ternary systems, water/alcohol/alcohol, water/alcohol/hydrocarbon, water/alcohol/CO_2 and the constituent subsystems (Li and Englezos, 2003; Li and Englezos, 2004). In this work, we applied the above SAFT for the prediction of the thermodynamic inhibiting effect of methanol, glycerol, ethylene glycol and triethylene glycol on gas hydrate formation. The vapor and liquid phases are described using the SAFT model. The van de Waals-Platteeuw model is used for the solid hydrate phase. In addition, the compositions of the equilibrium phases are calculated. It is noted that there are no applications of SAFT to gas hydrate formation so far.

2.4. Research objectives

Knowing hydrate phase equilibrium data for systems containing thermodynamic inhibitors also still incomplete, thus more experimental data for the systems containing inhibitors are required. Also a more powerful prediction model is need. My specific research objectives are:

- Measuring the incipient equilibrium hydrate formation data for CH_4-C_2H_6 and CH_4-C_3H_8 hydrates in the presence of triethylene glycol and glycerol.
- Predicting hydrate formation condition using Trebble-Bishnoi, and SAFT equations of state.

3, Materials, Apparatus and Methods

3.1. Materials

De-ionized water was used to avoid the contamination of unwanted salt during the experiments. Distilled water was used as the input to the water purifier to produce de-ionized water. The purity of de-ionized water was very important in this experiment because salts in the water such as NaCl, CaCl are inhibitors and will affect the measurements. Triethylene glycol was obtained from Sigam-Aldrich Canada, Ltd. The purity was 99%. Glycerol with 99.7% purity was obtained from Fisher Scientific.

The dry gas composition of the CH_4-C_2H_6 (C1-C2) mixture and the CH_4-C_3H_8 (C1-C3) mixture from cylinders were determined by Gas Chromatography prior to starting the experiments. The calibration procedure is shown in the Appendix C. The methane content found to be 91.0% and the balance ethane in the C1-C2 gas cylinder. The methane content of the C1-C3 cylinder was 90.5% and the balance propane.

3.2. Apparatus

All the experiments were carried out using the apparatus shown in Fig. 2. The equilibrium cell is made of Plexi-glass. The cell is immersed in a temperature-controlled bath. The liquid in the water bath is a mixture of water and ethylene glycol (50%-50%) to maintain a constant temperature within the system. The temperature of the glycol mixture is controlled by an external refrigerator/heater (VWR Scientific, MODEL 1187). The solution in the refrigerator/heater is a mixture of glycol and water which is circulated in a closed loop and exchanges heat with the solution inside the bath where the cell is immersed. Copper tubing was used for the construction of the heater/cooling coil. A motor-driven stirring mechanism was used to maintain a relatively constant temperature (±0.10K) in the bath over a long period of time. A digital pressure indictor (HEISE Digital Pressure Indictor) was connected to equilibrium cell to measure the pressure of the system. The maximum pressure the digital indictor can measure is 10000 psi with ± 0.07% F.S. (Full scale) accuracy. The gas in the equilibrium cell can be transported using sampling tube to Gas Chromatography (Varian GC CX3400) to analyze the gas composition. The hydrate formation and decomposition process can be observed through the

Microscope (NIKON, SMZ-2T) which is situated in front of the water bath. It provides more accurate observation with 5 times magnification.

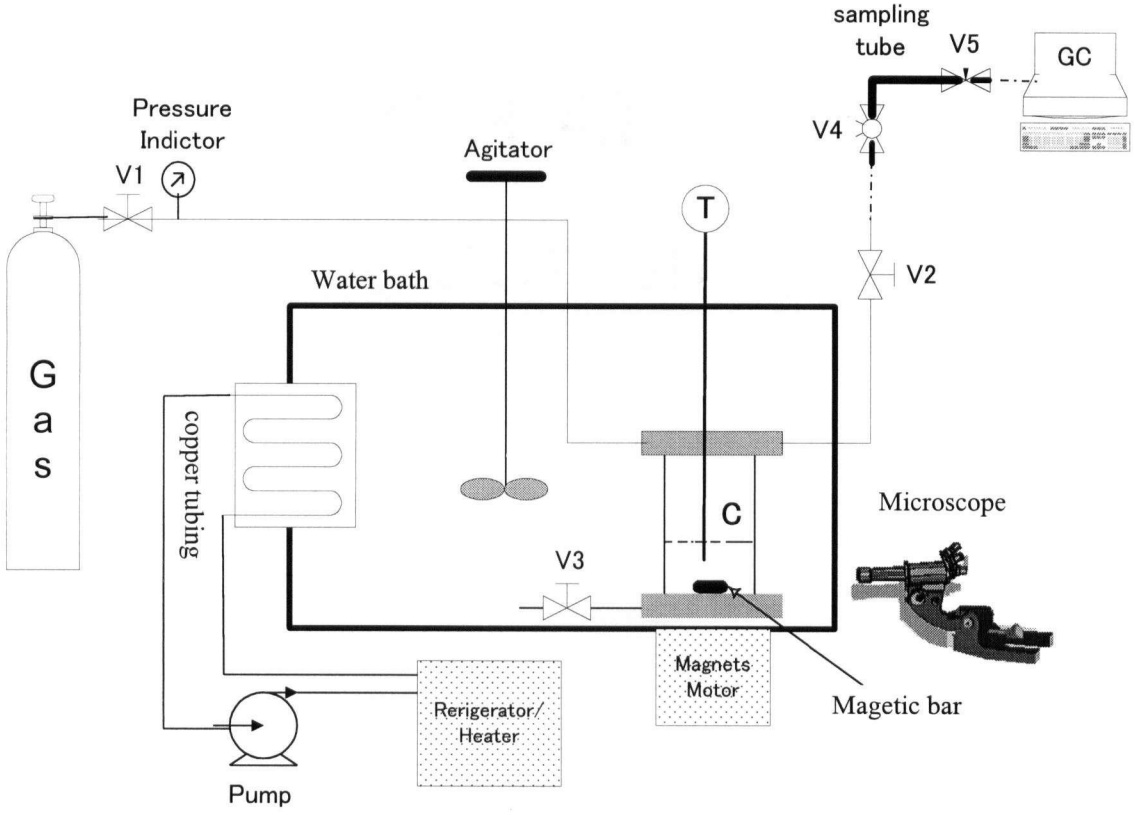

C: Equilibrium cell
T: Thermocouple
GC: Gas chromatography
V1,V2,V3,V4,V5: Valves

Figure 2: Schematic of the apparatus

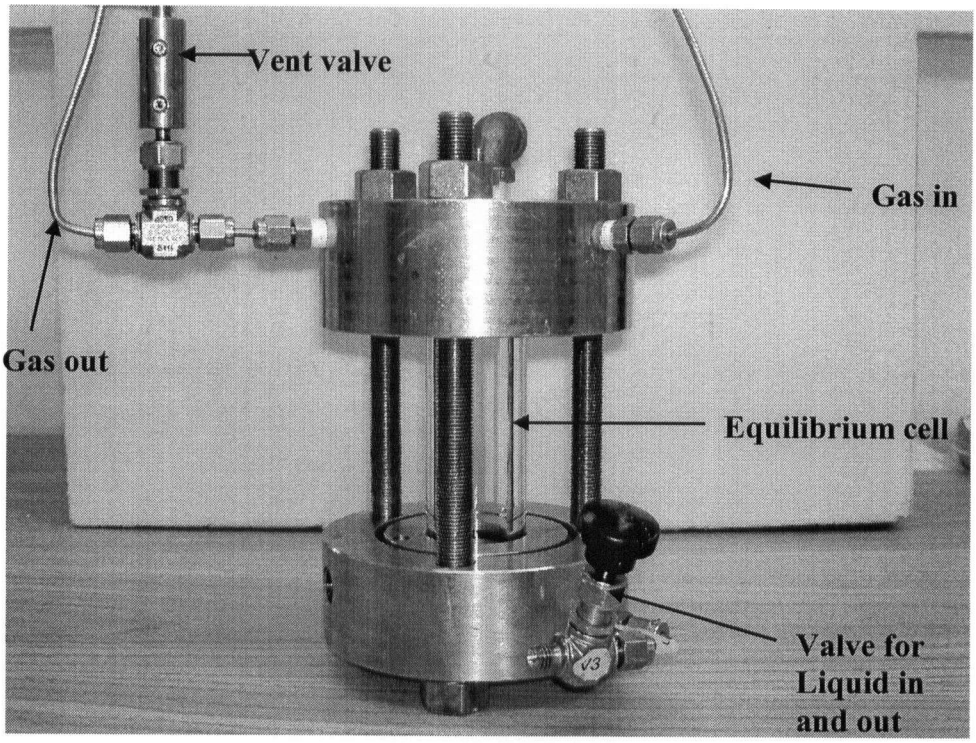

Figure3: photo of the equilibrium cell used in the experiments

The equilibrium cell is made from plexiglass with the dimensions of 25 mm (diameter)*44mm (height). Thickness of the cell is 6mm. This column has stainless steel lids on both sides which are held in place by 3 stainless steel bolts. Four neoprene O-rings were used to seal the lids. Figure 3 shows the photo of the equilibrium cell used in the experiments. Stirring of the cell contents is accomplished by using a magnetic stir bar coupled to a set of magnets underneath the equilibrium cell. The temperature inside the cell is measured with a copper-constant thermocouple from Omega which is placed just below the liquid surface. The accuracy of the thermocouple measurements is believed to be ±0.1K. The pressure is measured by HEISE Digital Pressure Indictor which is calibrated by an accurate pressure gauge (WIKA 27888DA). The pressure range is 0-10000psi and the accuracy of the pressure measurements is± 0.07% F.S.

A Varian gas chromatography model CX-3400 was used for measuring gas composition of C1-C2 (or C3)-(0%, 20.0%) TEG hydrate formation systems, and Varion model CP-3800 for C1-C2 (or C3)-30.0%TEG and C1-C2 (or C3)-20.0% Glycerol systems. Thermal Conductivity

(TCD) and Flame Ionization detectors (FID) are available in both chromatographs. Figure 4 shows the picture of the CP-3800 GC used in the experiments. During the experiments, the FID with a split injector was used to analyze the gas phase composition. The main parameters of GC were set as follows:

- The temperature of the injector: 150 °C
- The temperature of column: 40°C
- The temperature of the FID: 250 °C

Figure 4: the photo of the CP-3800 Gas Chromatograph used in the experiments

Water purifier (ELGA UHQ II, Great Britain) is used to product de-ionized water. The purity of de-ionized water was very important in this experiment because some salt in the water act as inhibitors, such as NaCl, CaCl, which affect the measurement result. The picture is shown in figure 5 as follow:

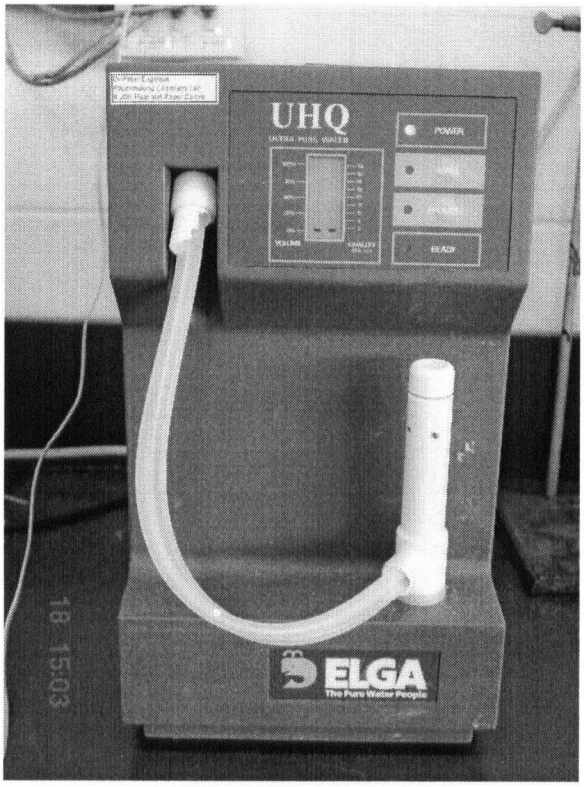

Figure 5: Water purifier ELGA UHQ II

Stirring of the contents of the equilibrium cell is accomplished by a magnetic stirring system (MODEL 200 MINI-STIRRER) and shown in figure 6.

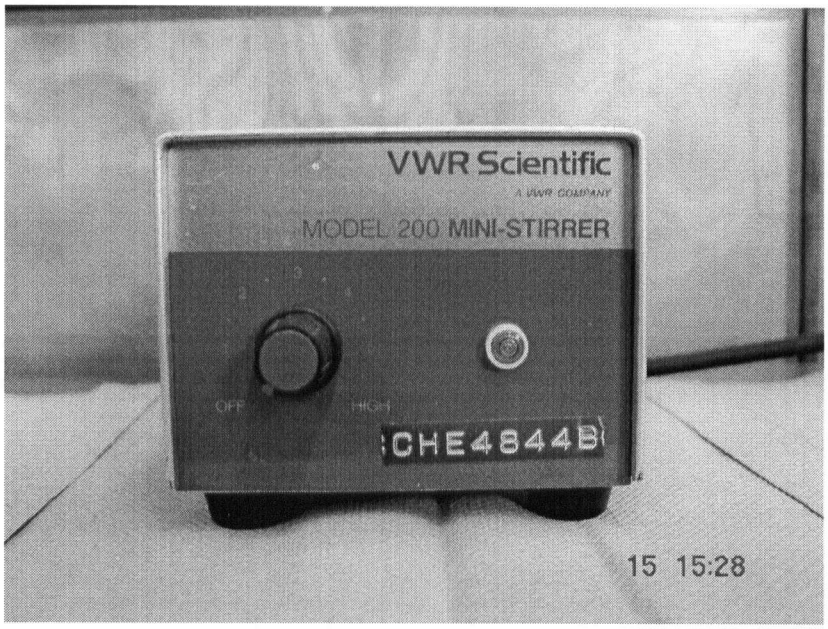

Figure 6: Magnetic stirring system (MODEL 200 MINI-STIRRER)

Figure 7 shows the picture of the sampling tube which was used in the experiments to collect the samples under equilibrium conditions and then inject it to the GC for analysis.

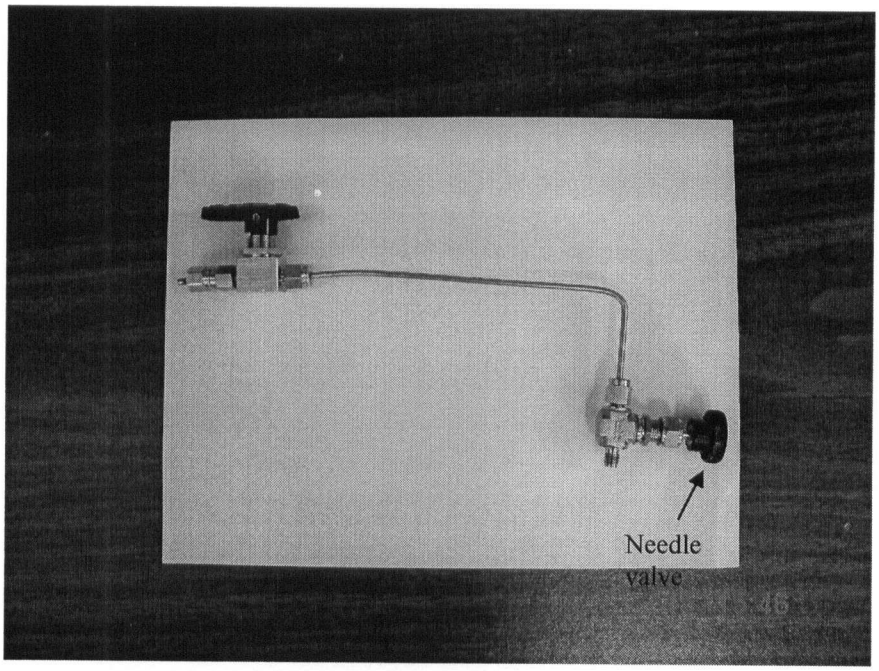

Figure 7: Sampling tube

3.3. Isothermal pressure search method

Incipient equilibrium conditions refer to the situation where an infinitesimal amount of hydrates is in equilibrium with the aqueous liquid phase and with the hydrocarbon-rich vapor phase. Practically, this is the situation when a small number of very tiny crystals (visible by a microscope) coexist in equilibrium with the fluid phases.

The isothermal pressure search method is used for the determination of the hydrate formation conditions (Englezos and Ngan, 1994). This method is used because the system can reach thermal equilibrium faster compared to the time required for an adjustment of the temperature. It is described next.

3.3.1 Estimation of the hydrate formation pressure

In order to facilitate the experimental search the equilibrium pressure values were roughly estimated based on available data. The following is an example on how to estimate the equilibrium pressures for system C1 (90.4%)-C2 (9.6%)-TEG (20.2%)-H2O. The phase diagram for the systems of C1-H2O, C1-TEG (20.2%)-H2O and C1 (90.4%)-C2 (9.6%)-H2O is shown on Figure 8. For example, to estimate equilibrium pressure at 278.0 K, a vertical line is drawn through the point at T=278.0K. It goes through the phase boundary lines of the systems C1-H2O, C1-TEG (20.2%)-H2O and C1 (90.4%)-C2 (9.6%)-H2O. As shown in the figure, the equilibrium pressure for system C1 (90.4%)-C2 (9.6%)-TEG (20.2%)-H2O at T=278K is equal to the pressure at point D (P_D) plus the pressure difference P_A-P_B. Following the same method, other equilibrium points can be estimated. This estimation result will give us an approximation of the hydrate formation conditions to be measured and thus expedite the process.

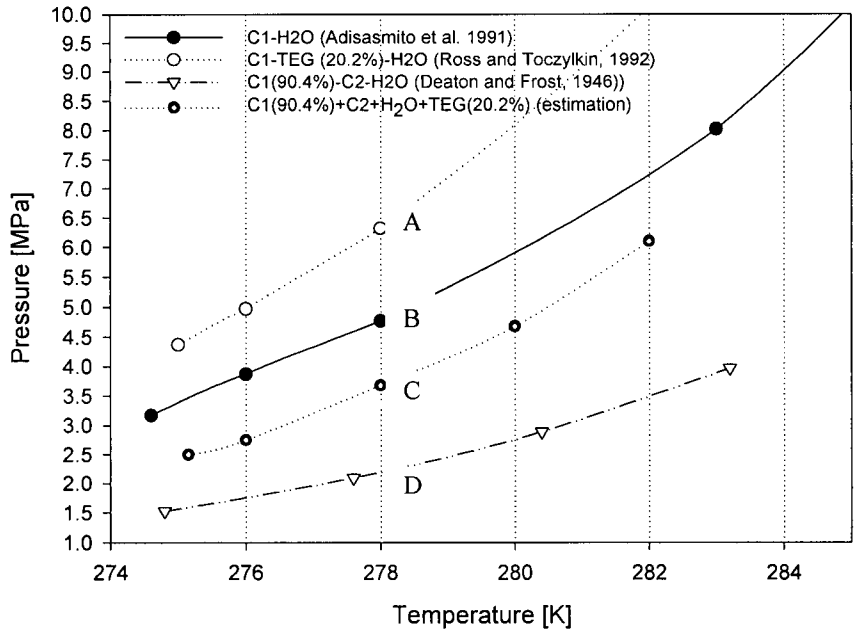

Figure 8. Roughly equilibrium pressure estimation for the system C_1-C_2-20.2%TEG-H2O

3.3.2 Solution preparation

During the experiments, 20.2%, 20.0 % and 30.0% (by weight) triethylene glycol solution and 20.0% glycerol solution are needed. Triethylene glycol and glycerol are all miscible with water in all proportions at room temperature. The appropriate amounts of laboratory grade TEG or

glycerol and deionized water were weighed using Mettler P2000 balance from Bracewell Balance and Inst. Service LTD with readabilities of 0.1mg. Then the solution was stirred for 30min for complete mixing.

3.3.3 Elimination of hydrate hysteresis phenomena

Before starting the measurements of the incipient formation pressures at different temperatures using a particular TEG or glycerol solution, hydrate formed and decomposed in order to eliminate the hysteresis phenomenon associated with hydrate formation. The procedure involves injecting 18ml of the aqueous TEG or glycerol solutions into a thoroughly cleaned cell. The solution was then allowed to reach a target temperature. Hydrate-forming gas at the pressure 2000KPa was then injected into the cell and removed. The magnetic stirring system is then started. Subsequently, the cell was pressurized above the hydrate formation pressure to form large amount of hydrate. Next; the hydrate crystals were decomposed by venting the gas out of the cell. It is necessary to repeat this procedure at least twice to eliminate the hydrate hysteresis phenomena.

3.3.4 Hydrate formation condition measurement

After eliminating the hydrate hysteresis phenomena, the cell was pressurized around the estimated hydrate formation pressure and the system was allowed to reach the target temperature. After that, the cell pressure was further increased by introducing more gas into the cell to induce hydrate nucleation. The pressure was set well above the hydrate formation point in order to have a large driving force and induce hydrate nucleation quickly. Once a small amount of hydrate was formed, the pressure was quickly decreased to the expected equilibrium value (estimated as shown in figure 5) by venting some of the gas out of the cell. If this small amount of tiny hydrate in the system were still present after at least four-hour period, the pressure was recorded. Then the pressure was dropped by about 50KPa. If the hydrate in the cell completely decomposed, the recorded pressure is taken as the equilibrium hydrate formation pressure at this temperature. If the hydrate was not present after the four-hour period, the pressure of the system was below the equilibrium pressure. In this case, the experiment was repeated but the new estimated equilibrium pressure was set at a higher value (50KPa above). The experiment was terminated when the

pressure and temperature in the cell were constant and an infinitesimal amount of hydrate crystals was detectable with the aid of the microscope.

4. Experimental Results and Discussion

4.1 Validation of experimental apparatus and procedure

In order to establish the validity of the experimental apparatus, two experiments were performed with methane and water and the results were compared with the data available in the literature. The numerical values of the measured data and those from the literature are shown in Table 2. In figure 9, the literature data together with the experimental data obtained in this work are shown. From figure 9, we can see that our measurements compare well with those from the literature.

Table 2. Experimental data from this work and literature on methane hydrate formation in pure water solution (Adisasmito. et al., 1991)

T/K	Experiment Pressure/MPa	
	Adisasmito, 1991	This work
273.4	2.68	
274		2.94
274.6	3.05	
276.7	3.72	
278.3	4.39	
279.6	5.02	
280.4		5.53
280.9	5.77	
282.3	6.65	
283.6	7.59	
284.7	8.55	
286.4	10.57	

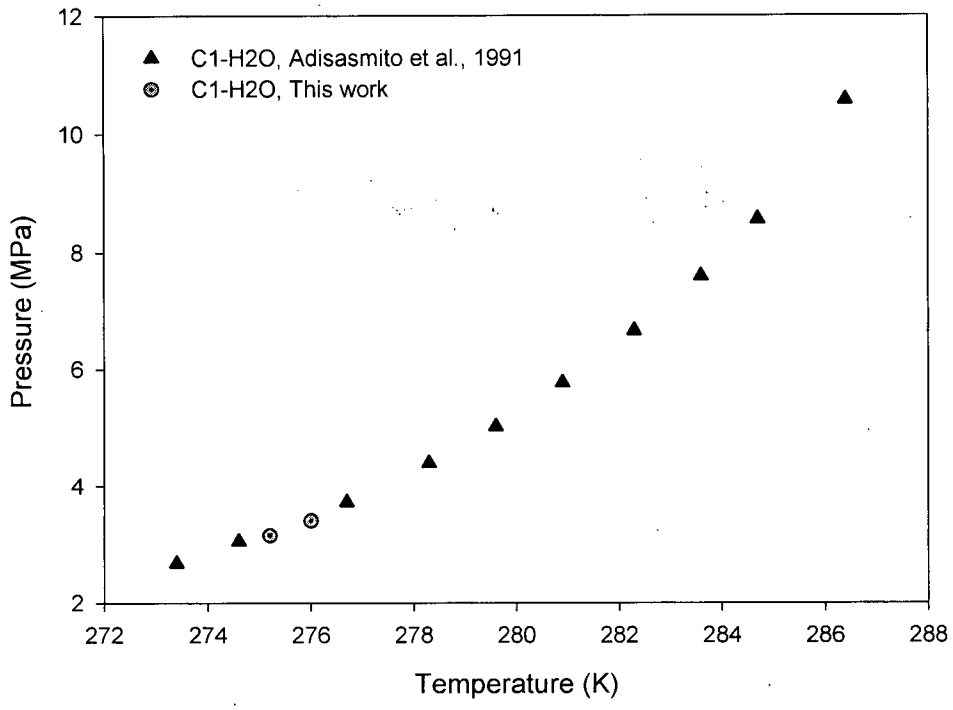

Figure 9. Comparison of experimental data obtained in this work and data from Adisasmito

4.2 Incipient equilibrium data on methane (C1)-ethane (C2) hydrate formation in aqueous TEG solutions

After the validation of the apparatus and the procedure, the incipient hydrate formation conditions for the C1-C2-TEG-H2O system were measured. The concentrations of TEG in the aqueous solution are 20.2wt% and 30wt%. The results are shown in table 3 and plotted in figure 10. In order to obtain a measure of the inhibition ability of TEG, two incipient hydrate formation data for the C1-C2-H2O system with the same C1 and C2 gas composition were measured, and results are given in table 4 and shown in figure 10 as well. The solid lines shown in the figure are drawn by "best fit" to clarify the trends of the data. As seen from figure 10 TEG shows considerable inhibition ability on C1-C2 hydrate formation. The inhibiting effect is also proportional to the concentration of the inhibitor.

Table 5 shows the hydrate point depression for each concentration at three different pressures (Appendix I gives the explanation on how to calculate the hydrate point depression).

However, the experimental uncertainty is greater than the differences in hydrate point depression for aqueous TEG solution at different pressures, so it was assumed that the hydrate point depression values are not significantly affected by pressure. Table 5 also shows the change in hydrate point depression for increasing concentrations of TEG at 2500kPa.

The gas composition was measured using GC, the results is also given in table 3 and shown in figure 11. From the figure, we can see that gas composition in equilibrium condition has changed somewhat compared with the original gas composition from the cylinder. The C1 concentration increased and C2 concentration decreased. This is consistent with the fact that C2 is more soluble than C1 in the water phase

Table 3. Incipient equilibrium hydrate formation conditions and gas phase molar composition for the C_1-C_2 (9.0%)-TEG (20.2% and 30.0%)-H_2O system

Concentration of TEG (mass %)	Temperature/K	Pressure/MPa	Gas mole fraction	
			C1	C2
20.2%	282.0	4.458	91.4	8.6
	280.8	3.858	91.4	8.6
	279.5	3.280		
	276.5	2.430	91.4	8.6
	274.9	2.087	91.4	8.6
	272.6	1.528	91.5	8.5
30.0%	280.2	4.520		
	279.4	4.130	90.8	9.2
	277.4	3.400	90.7	9.3
	275.3	2.800	90.9	9.1
	273.8	2.280	90.9	9.1

Table 4. Incipient equilibrium hydrate formation conditions data for the C_1-C_2 (9.0%)-H_2O system

Temperature/K	Pressure/MPa
279.6	2.700
276.8	1.928

Table 5. Hydrate point depression (ΔT_H), and change in hydrate point depression at 2500 kPa ($\Delta T_{H, 2500}$) in TEG-water

Concentration of TEG (mass %)	(ΔT_H/K)			($\Delta T_{H, 2500}$)/K
	P=2500kPa	P=3000kPa	P=3500kPa	
0	0	0	0	
20.2	2.3	2.3	1.8	2.3
30	4.7	4.7	4.4	2.4

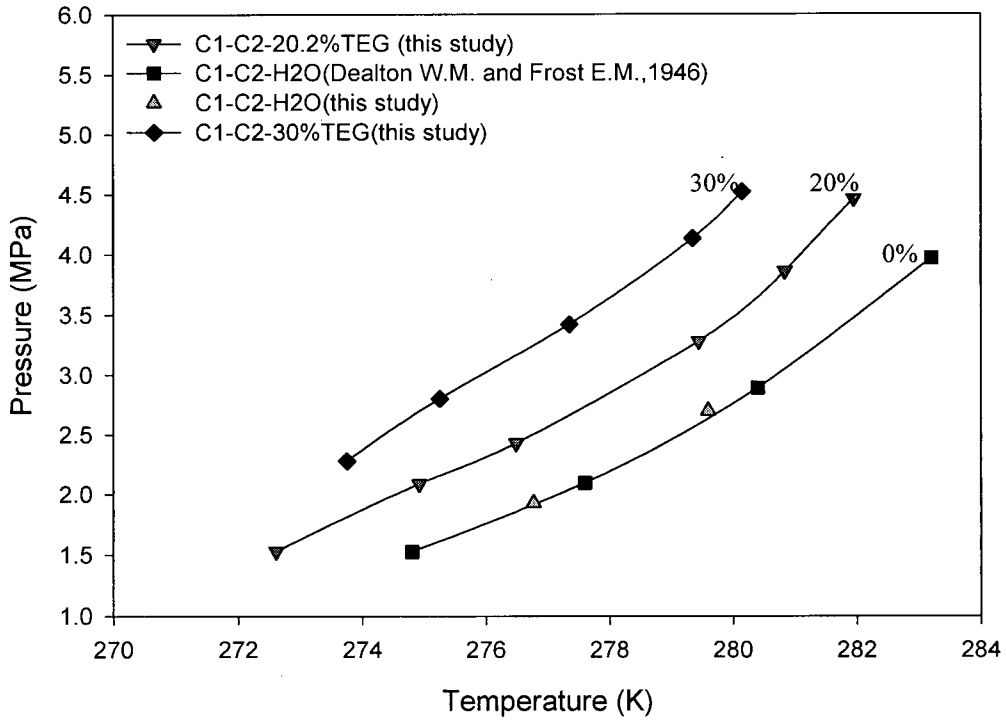

Figure 10: Equilibrium data on C1-C2 hydrate formation in water-triethylene glycol solutions

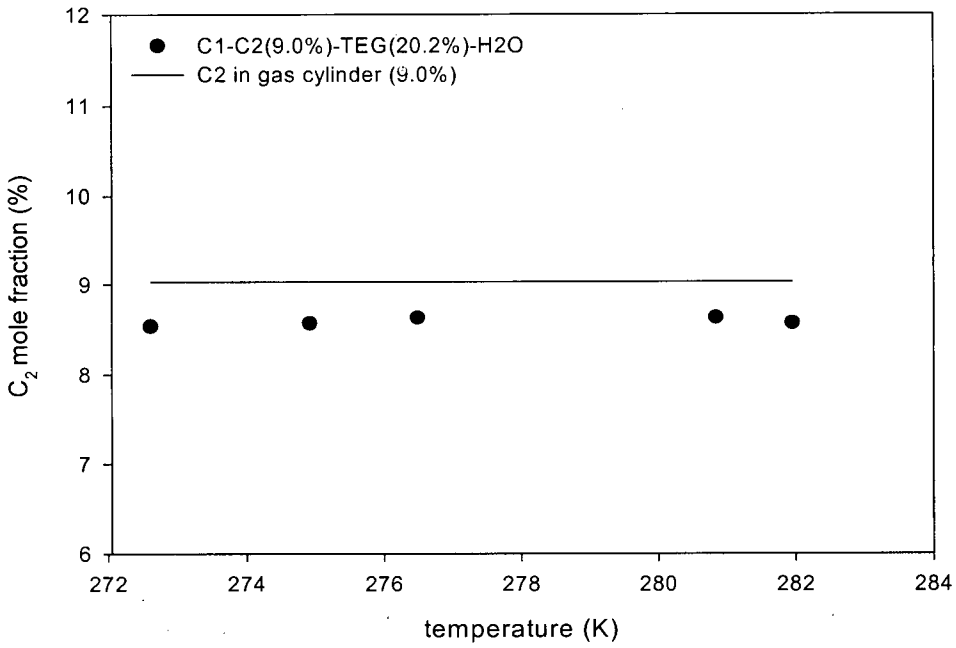

Figure 11: C2 mole fraction at each equilibrium condition

4.3. Incipient equilibrium data on methane-propane (C3) hydrate formation in aqueous TEG solutions

The incipient hydrate formation conditions for methane and propane mixture (methane is 90.5% and propane is 9.5% by volume) in aqueous 20.2 and 30 wt% TEG solution and in pure water were measured and the results are given in Table 6. The data are also plotted and shown in Figure 12. The solid lines shown in the figure are drawn by "visual fit" to clarify the trends of the data.

Figure 12 clearly shows the inhibiting effect of TEG in methane-propane hydrate formation conditions. The hydrate point depressions for each concentration at three different pressures are obtained and shown in the table 7. The change in hydrate point depression for increasing concentrations of glycerol at 1000kPa is also shown in the table.

The gas composition at each equilibrium condition was also obtained and the results are shown in Table 6. The comparison between propane mole fractions at each equilibrium conditions with the propane mole fraction from the original gas cylinder is plotted in Figure 13. As seen in the figure the gas composition changes compared to the original gas composition from the gas cylinder. The methane concentration increased whereas the propane one decreased because propane is more soluble than methane. Moreover, we can see that the solubility of propane in TEG solution is more than that in the pure water. Finally the gas composition does not change compared to the original gas form the cylinder for the 30% TEG solution.

Table 6. Incipient equilibrium hydrate formation conditions data and gas phase molar composition for the C_1-C_3 (9.5%)--H_2O and C_1-C_3 (9.5%)-TEG (20.0% and 30%)-H_2O system.

Concentration of TEG (mass %)	Temperature/K	Pressure/KPa	Gas mole fraction	
			C_1	C_3
0	280.6	1190.4		
	278.9	990.4		
	277.0	783.4	90.6	9.4
	275.4	645.0	90.6	9.4
	273.6	521.6	90.4	9.6
20	281.4	1756.0	91.6	8.4
	279.5	1418.0	91.4	8.7
	277.3	1142.1	91.6	8.4
	275.4	915.0	90.9	9.1
	273.6	750.0		
30	281.7	2211	90.3	9.7
	280.0	1831		
	277.8	1390	90.1	9.9
	276.0	1120	90.5	9.5
	274.2	900		

Table 7: Hydrate point depression (ΔT_H), and change in hydrate point depression at 1000 kPa ($\Delta T_{H,\,1000}$) in TEG-water

Concentration of TEG (mass %)	(ΔT_H/K)			($\Delta T_{H,\,1000}$)/K
	P=900kPa	P=1000kPa	P=1190kPa	
0	0	0	0	
20	2.7	2.8	3.0	2.8
30	3.9	4.1	4.4	1.3

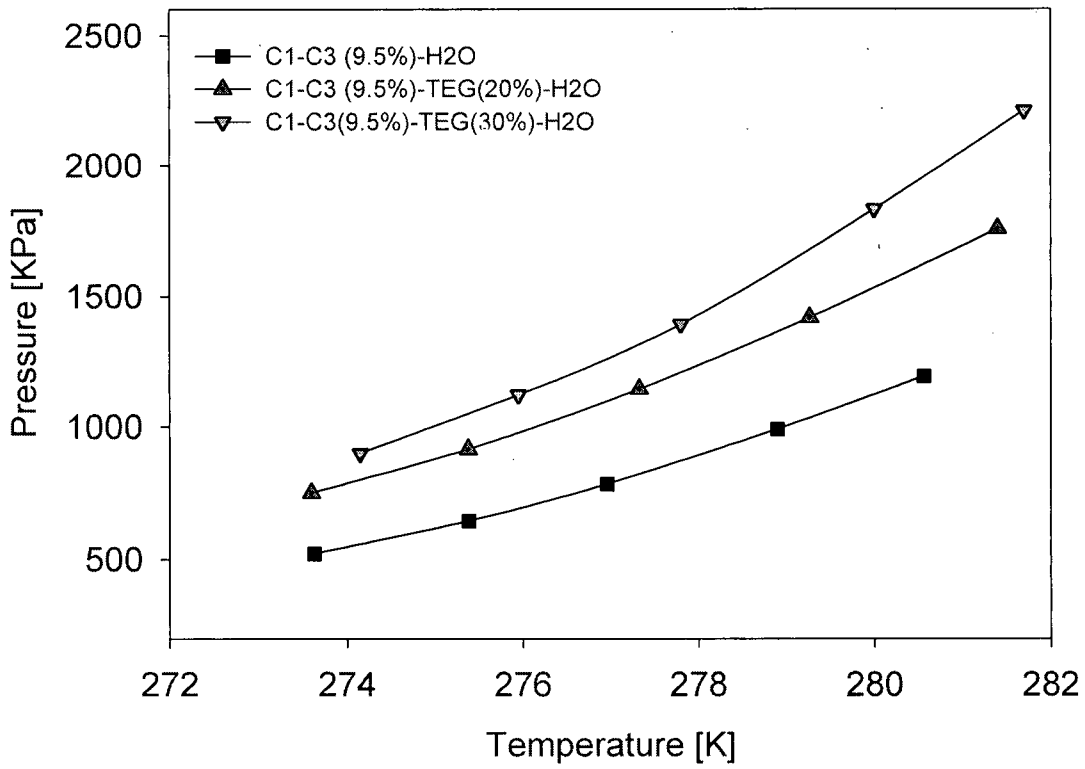

Figure 12: Equilibrium data on C1-C3 hydrate formation in water-triethylene glycol solution

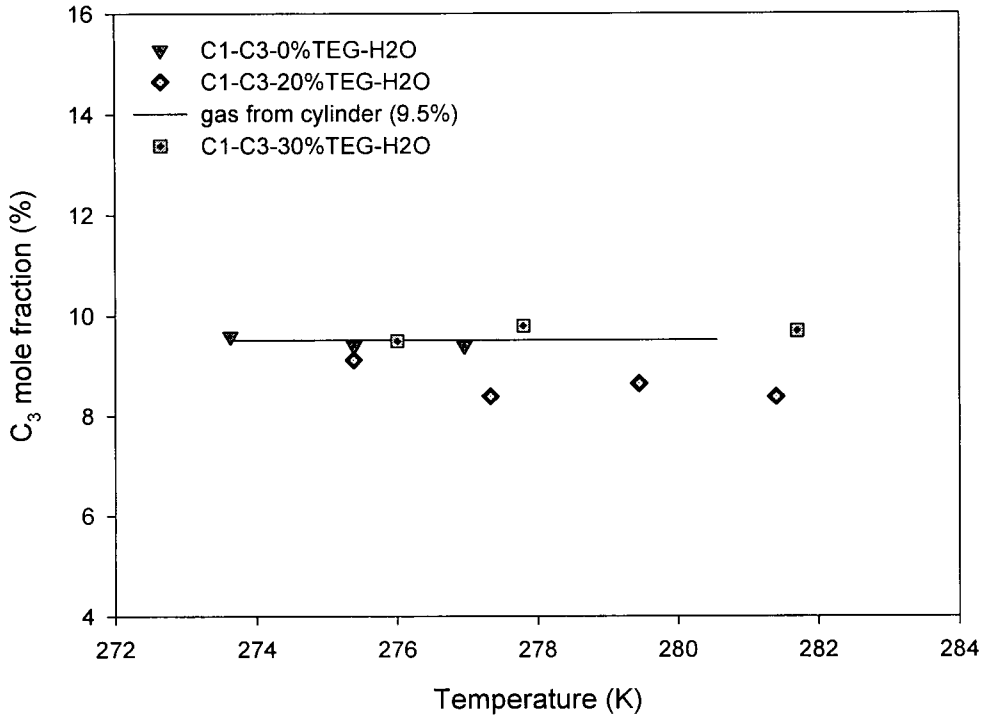

Figure 13: C3 mole fraction at each equilibrium condition

4.4. Incipient Equilibrium Data on Methane (C1)-Ethane (C2) Hydrate Formation in Aqueous Glycerol Solutions

The incipient hydrate formation conditions for the methane-ethane mixture (methane is 91.0% and propane is 9.0% by volume) in 0% and 20wt% aqueous Glycerol solutions were measured and the results are given in Table 8. The data are also plotted and shown in Figure 14.

It is obvious that glycerol also has a considerable inhibiting effect in hydrate formation. The hydrate point depression for each concentration at three different pressures is shown in the table9. As seen the hydrate point depression at a given inhibitor concentration is independent of pressure.

The gas composition at each equilibrium condition was also obtained. The results are shown in Table 8. The comparison of C2 mole fractions at each equilibrium condition with the C2 mole fraction in the original gas cylinder is plotted in Figure 15. As seen the gas composition at each equilibrium condition does not change significantly compared to the cylinder gas composition.

Table 8: Incipient equilibrium hydrate formation conditions data and gas phase molar composition for the C_1-C_2 (9.0%)--H_2O and C_1-C_2 (9.0%)-Glycerol (20.0%)-H_2O system.

Concentration of Glycerol (mass %)	Temperature/K	Pressure/KPa	Gas mole fraction	
			C_1	C_2
0	279.6	2.700		
	276.8	1.928		
20	274.2	2130	90.9	9.1
	276.3	2620	91.1	8.9
	278.8	3420	90.8	9.2
	280.1	4100		
	281.3	4751	90.8	9.2

Table 9. Hydrate point depression (ΔT_H) of Glycerol-water system.

Concentration of Glycerol (mass %)	(ΔT_H/K)		
	P=2200kPa	P=2400kPa	P=2600kPa
0	0	0	0
20	3.3	3.2	3.0

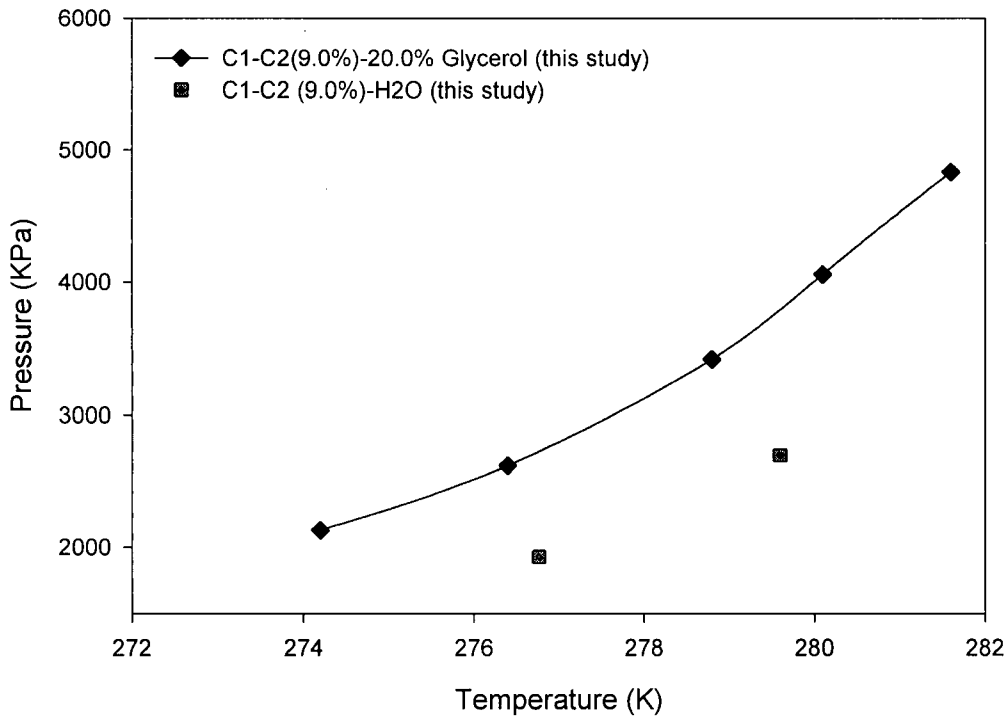

Figure 14: Equilibrium data on C1-C2 hydrate formation in water-Glycerol solution

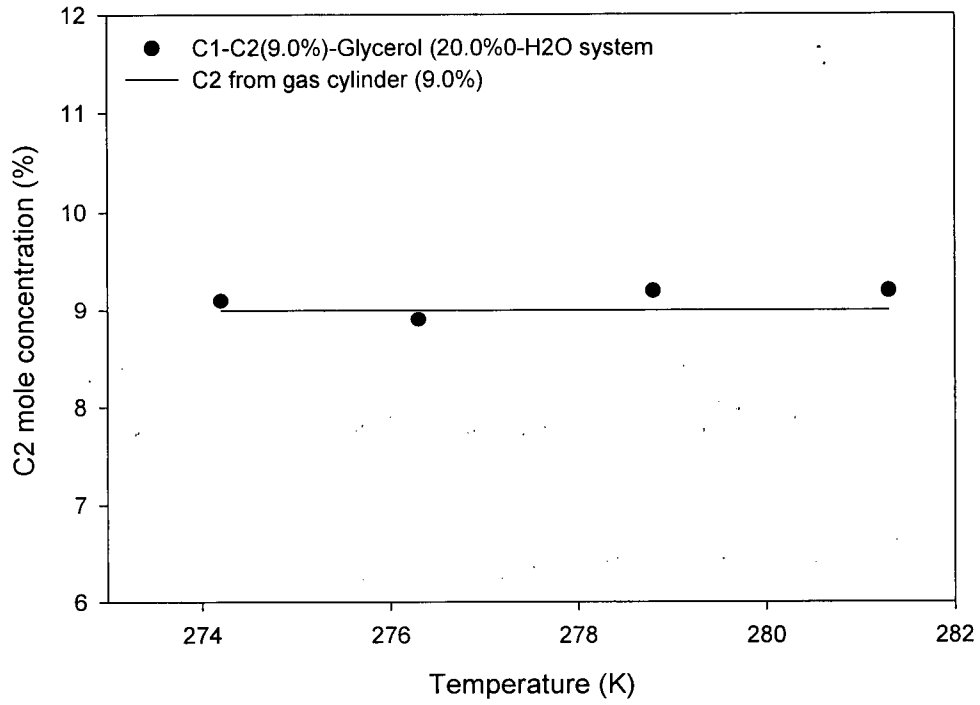

Figure 15: C2 mole fraction at each equilibrium condition in water-glycerol solution

4.5. Incipient Equilibrium Data on Methane (C1)-Propane (C3) Hydrate Formation in Aqueous Glycerol Solutions.

The incipient hydrate formation conditions for the system of C1-C3 (9.5%)-20.0% glycerol-H2O were measured as well. The results are shown in the table11 and plotted in the figure 16. The hydrate point depression at three different pressures is shown in table 11. It can be assumed that the hydrate point depression values are not affected by pressure at the same concentration.

The gas composition at each equilibrium condition is obtained using GC and the results are shown in Table 6 as well. The comparison of C2 mole fractions at each equilibrium conditions with the C2 mole fraction from the original gas cylinder is plotted in Figure 17.

Table 10. Incipient equilibrium hydrate formation conditions data and gas phase molar composition for the C_1-C_3 (9.5%)--H_2O and C_1-C_3 (9.5%)-Glycerol (20.0%)-H_2O system

Concentration of Glycerol (mass %)	Temperature/K	Pressure/KPa	Gas mole fraction	
			C_1	C_3
0	273.6	522		
	275.4	645		
	277	783	90.6	9.4
	278.9	990	90.6	9.4
	280.6	1190	90.4	9.6
20	274.2	870	90.0	10.0
	275.7	1020	90.0	10.0
	278.3	1330	90.1	9.9
	280.3	1690	90.1	9.9
	281.6	1990		

Table 11: Hydrate point depression (ΔT_H) of Glycerol-water system

Concentration of Glycerol (mass %)	(ΔT_H/K)		
	P=840kPa	P=1000kPa	P=1190kPa
0	0	0	0
20	3.2	3.2	3.4

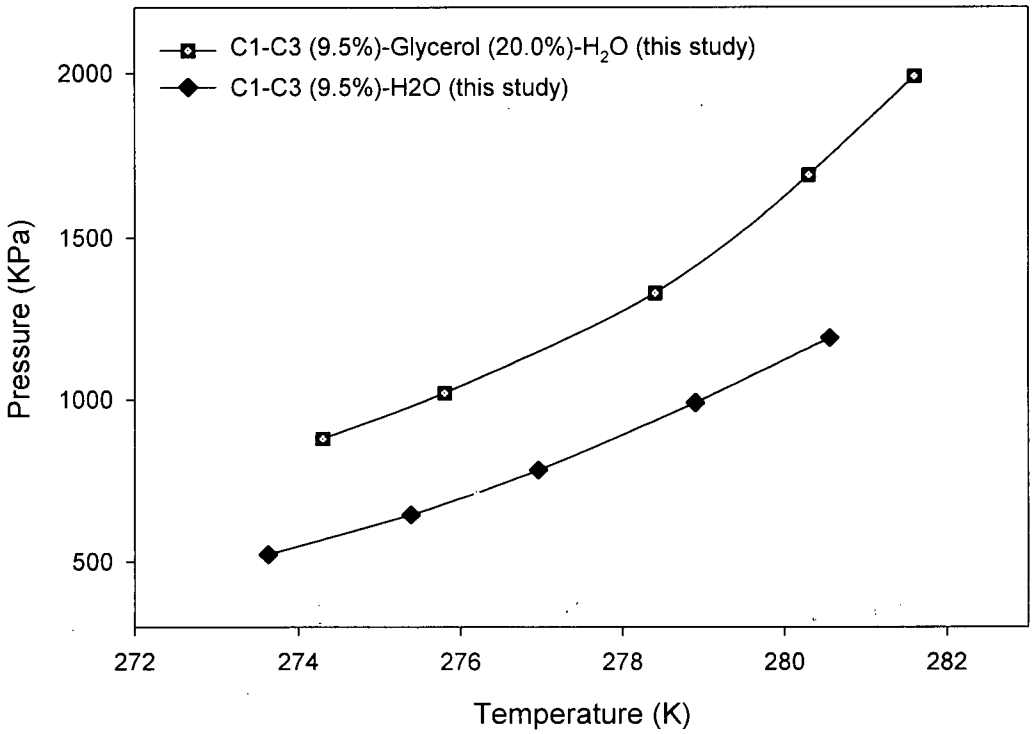

Figure 16: Equilibrium data on C1-C3 hydrate formation in water-glycerol solution

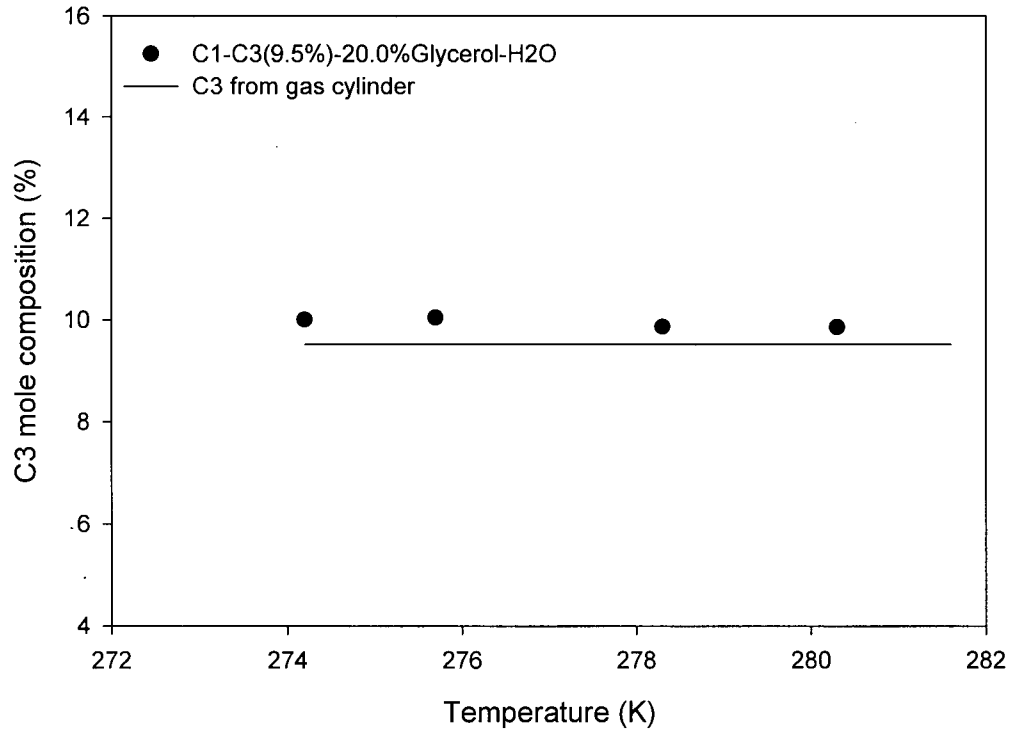

Figure 17: C3 mole fraction in each equilibrium condition in water-glycerol solution

5. Hydrate formation prediction using Trebble-Bishnoi equation of state (T-B EoS)

The well-known TB EoS is applied to predict the all above four-component hydrate formation systems (Trebble and Bishnoi, 1988). The methodology of the calculation has been presented in details elsewhere (Englezos et al. 1991). The binary interaction parameters for the equation are shown in the table 12. The computational flow diagram is shown in the figure 18 (Englezos et al. 1991). The predictions are compared to the experimental results and the absolute average deviation of predicted pressure (AAD (P), %) is defined as follows (Englezos et al. 1991)

$$AAD(P)(\%) = \left(\frac{1}{N_P}\right)\sum_{i=1}^{N_P}\left[\left|\frac{P_{cal} - P_{\exp}}{P_{\exp}}\right|\right]_i \times 100$$

where N_P is the number of data points

Table 12: Set of binary interaction parameters for each system

system	K_a	K_b	K_d	Literature source
H2O-CH4	0.4284	-0.1727	-1.2266	Englezos et al. (1991) Trebble and Bishnoi (1998) (binary interaction parameter)
H2O-C2H6	0	0	-0.2611	
H2O-C3H8	0	0	-0.2969	
CH4-C2H6	-0.0052	0	0	
CH4-C3H8	-0.0135	0	0	
TEG-CH4	-2.399	0	0.952	Jou and Otto (1987) (equilibrium data)
TEG-C2H6	0.299	0	-0.295	
TEG-C3H8	0.465	0.881	1.412	
H2O-TEG	0	0.854	0	Cartays and Starling (1996) (equilibrium data)

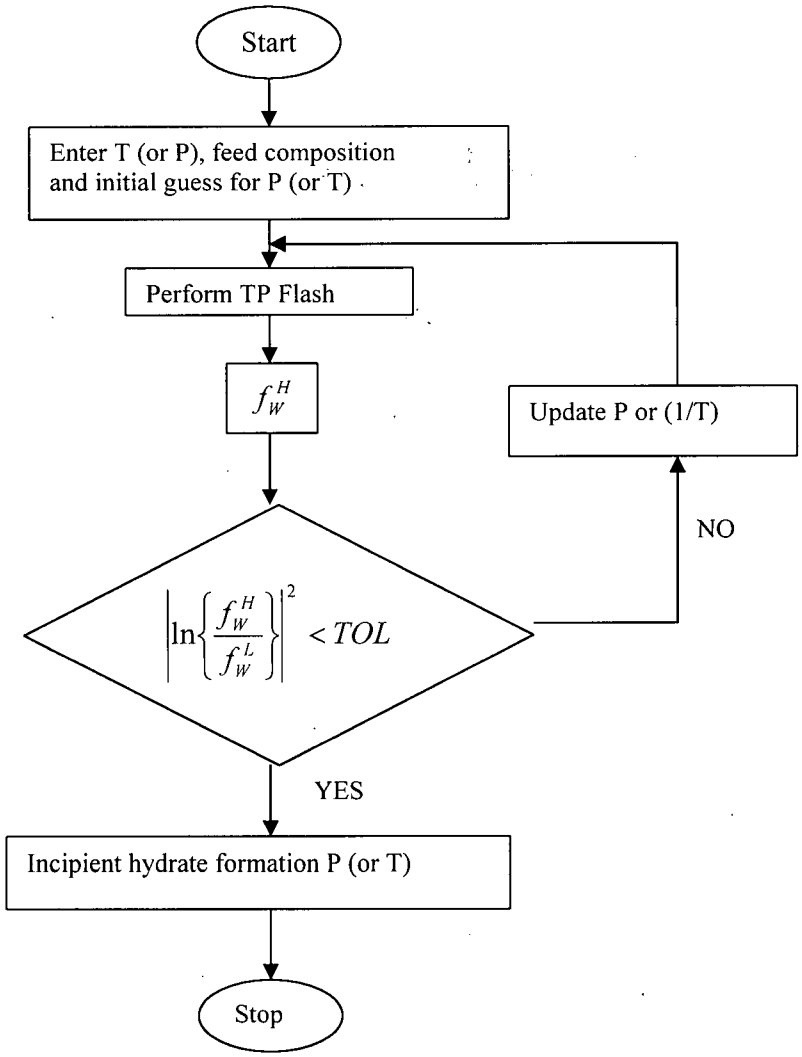

Figure 18: Computational hydrate formation P (or T)

5.1. Prediction of Methane (C1)-Ethane (C2) Hydrate formation in aqueous TEG solutions

Predictions of methane and ethane gas mixture hydrate formation systems with different concentrations of TEG using T-B equation of state were shown in the table 13 and plotted in the figure 19. It is obvious that the prediction is very good.

Table 13: experimental data and prediction of Methane (C1)-Ethane (C2) Hydrate formation in aqueous TEG solutions

Concentration of TEG (mass %)	Temperature (K)	P_{eq} (experiments) (MPa)	P_{eq} (prediction) (MPa)	AADP (%)
0	279.6	2.700		
	276.8	1.928		
20.2	282.0	4.458	4.67	4.0%
	280.8	3.858	3.97	
	279.5	3.280	3.31	
	276.5	2.430	2.52	
	274.9	2.087	2.18	
	272.6	1.528	1.64	
30.0	280.2	4.520	4.6	2.74%
	279.4	4.130	4.15	
	277.4	3.400	3.39	
	275.3	2.800	2.8	
	273.8	2.280	2.45	

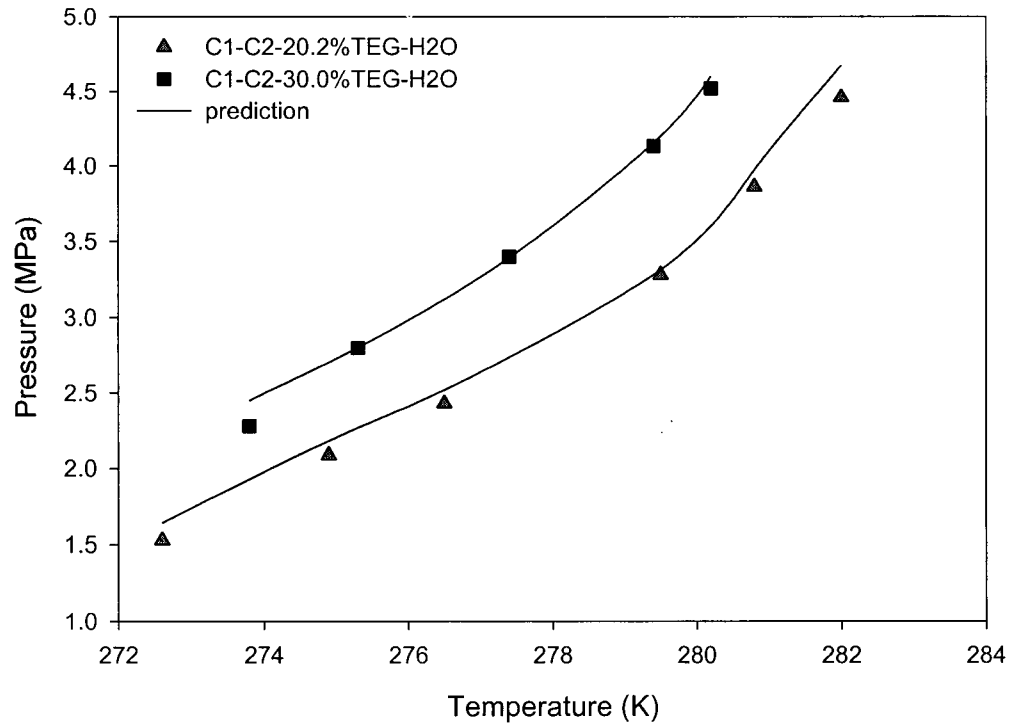

Figure 19: experimental data and predictions on C1-C2 hydrate formation in water-triethylene glycol solution

5.2. Prediction of Methane (C1)-Propane (C3) Hydrate formation in aqueous TEG solutions

Predictions of methane and propane gas mixture hydrate formation systems with different concentrations of TEG using T-B equation of state were shown in the table 14 and plotted in the figure 20.we can see that TB EoS gave prediction in good agreement with the experimental data.

Table 14: experimental data and predictions on C1-C3 hydrate formation in aqueous TEG solution

Concentration of TEG (mass %)	Temperature (K)	P_{eq} (experiments) (MPa)	P_{eq} (prediction) (MPa)	AADP (%)
0	280.6	1.19	1.18	1.06
	278.9	0.99	1	
	277.0	0.78	0.78	
	275.4	0.65	0.64	
	273.6	0.52	0.53	
20.0	281.4	1.76	1.74	1.91
	279.5	1.42	1.41	
	277.3	1.14	1.13	
	275.4	0.91	0.89	
	273.6	0.75	0.74	
30.0	281.7	2.21	2.2	0.86
	280.0	1.83	1.83	
	277.8	1.39	1.38	
	276.0	1.12	1.11	
	274.2	0.9	0.88	

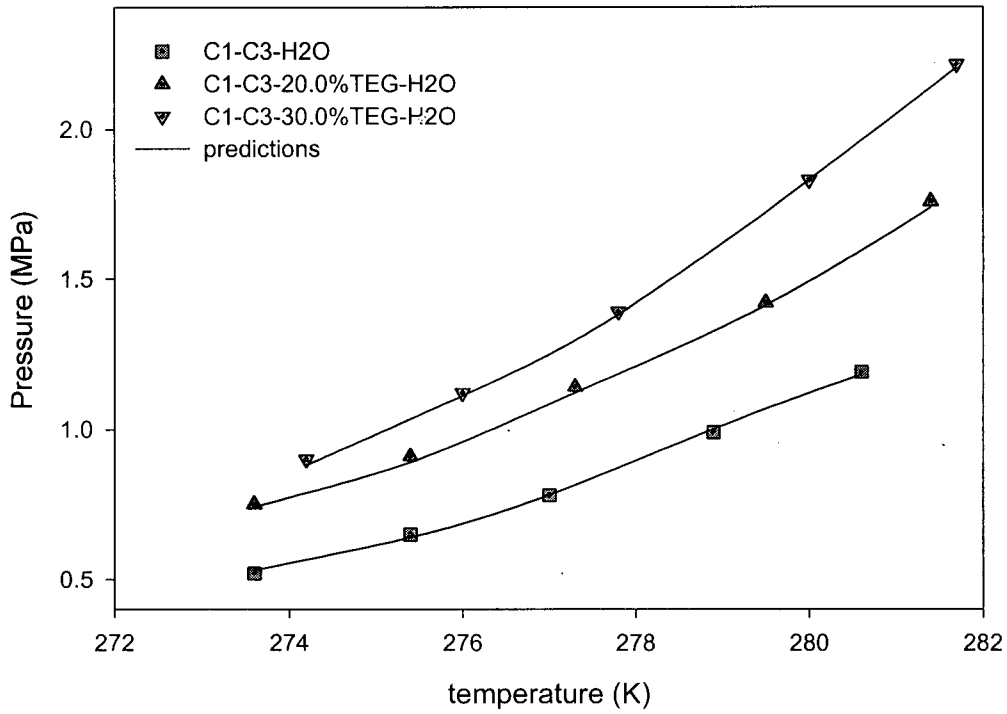

Figure20: experimental data and predictions on C1-C3 hydrate formation in water-triethylene glycol solution

5.3. Prediction of Methane (C1)-Ethane (C2) Hydrate formation in aqueous 20.0wt% glycerol solutions

The incipient hydrate formation conditions for C1-C2 (9.0%) gas mixture in the presence of 20.0wt% glycerol were predicted using TB EoS. The predictions were compared with the experimental data and shown in table 15 and plotted in the figure 21. From the figure, we can see that the prediction is very comparable with the experimental data. The AADP is only 0.85%.

Table 15: experimental data and predictions on C1-C2 hydrate formation in 20.0wt% glycerol solution

Temperature (K)	P_{eq} (experiments) (MPa)	P_{eq} (prediction) (KPa)	AADP (%)
274.2	2.13	2.15	0.85%
276.3	2.62	2.78	
278.8	3.42	3.63	
280.1	4.10	4.30	
281.3	4.75	4.90	

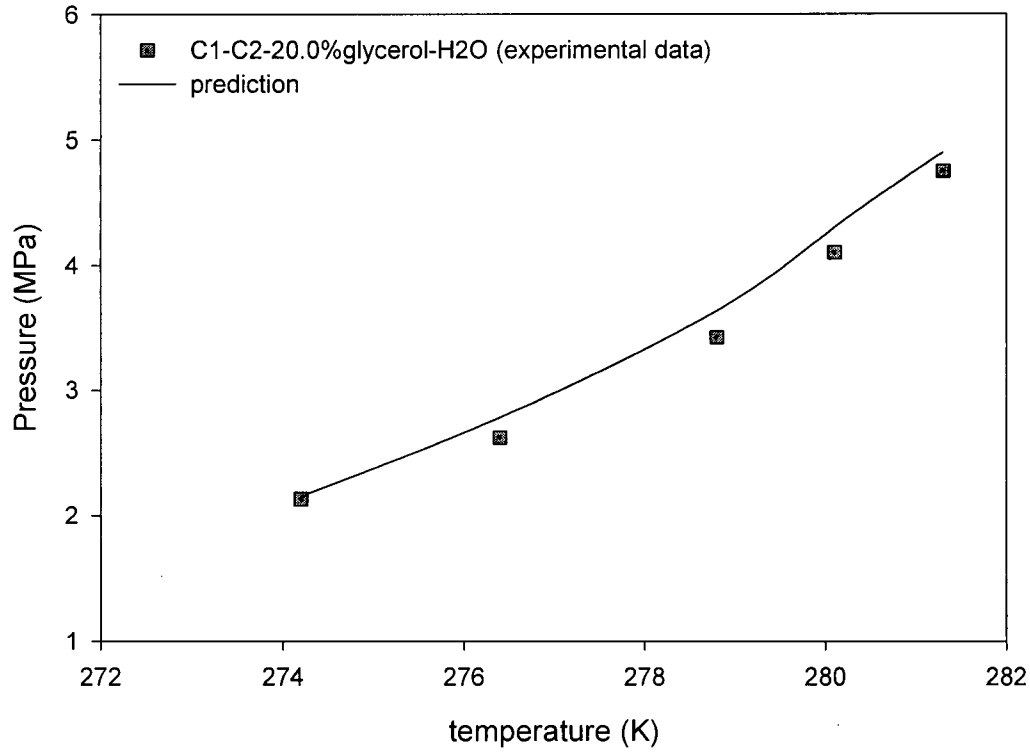

Figure 21: experimental data and predictions on C1-C2 hydrate formation in water- glycerol solution

5.4. Prediction of Methane (C1)-Propane (C3) Hydrate formation in aqueous 20.0wt% glycerol solutions

The incipient hydrate formation conditions for C1-C3 (9.5%) gas mixture in the presence of 20.0wt% glycerol were predicted using TB EoS. Table 16 compares the experimental data with the predicted values. It can be seen from figure 22 that the experimental data matches well with the predictions.

Table 16: experimental data and predictions on C1-C3 hydrate formation in 20.0wt% glycerol solution

Temperature (K)	P_{eq} (experiments) (MPa)	P_{eq} (prediction) (KPa)	AADP (%)
274.2	0.87	0.93	1.6%
275.7	1.02	1.10	
278.3	1.33	1.48	
280.3	1.69	1.82	
281.6	1.99	2.11	

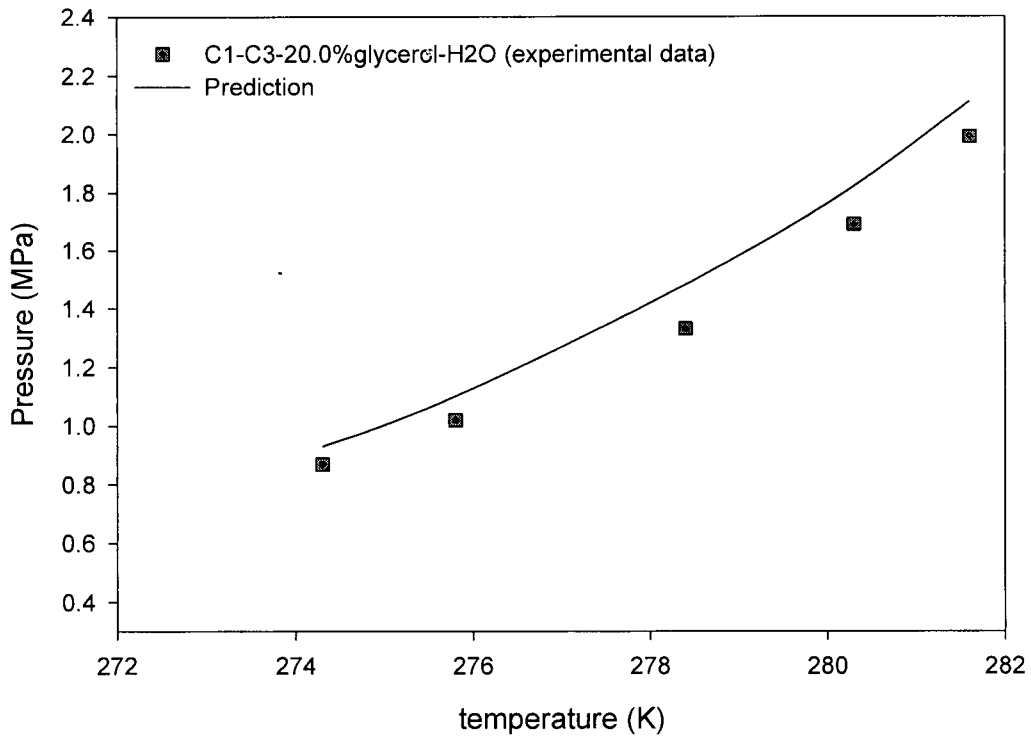

Figure 22: experimental data and predictions on C1-C3 hydrate formation in water- glycerol solution

6. Hydrate Formation Prediction using SAFT Equation of State

6.1. Thermodynamic Framework

In a system of N components containing solid hydrate (H), vapor (V) and liquid (L), the thermodynamic equilibrium is represented by,

$$f_i^L = f_i^V \qquad (i=1,...,N) \qquad (1)$$

$$f_j^H = f_j^V \qquad (j=1,...,n_c) \qquad (2)$$

where f is the fugacity of component i or j; N is all the components; n_c is the hydrate forming components including water.

In the above equations, the fugacities in vapor, liquid and solid phases may be calculated using a suitable thermodynamic model.

6.2. Equation of State for Vapor and Liquid Phases

In this work, the SAFT Equation of State is employed to predict the high-pressure vapor-liquid phase equilibrium (VLE) of water/gas/inhibitor systems.

The residual Helmholtz free energy for an n-component mixture of associating chain molecules can be expressed as the sum of hard sphere repulsion, hard chain formation, dispersion and association terms as follows

$$A^{res} = A - A^{id} = A^{hs} + A^{chain} + A^{disp} + A^{assoc} \qquad (3)$$

where A^{id} is the free energy of an ideal gas with the same density and temperature as the system, A^{hs} is the free energy of a hard-sphere fluid relative to the idea gas, A^{chain} is the free energy when chains are formed from hard spheres, A^{disp} and A^{assoc} are the contributions to the free energy of dispersion and association interactions, respectively. The molecules are described as homonuclear and chainlike. They are considered to be composed of spherical segments of equal-size and equal-interaction parameters with Lennard-Jones potential.

6.2.1 Hard-sphere repulsion term

The hard sphere term A^{hs} is calculated with the Boublik-Mansoori-Carnahan-Starling-Leland equation as follows (Boublik, 1970; Mansoori et al. 1971).

$$\frac{A^{hs}}{NkT}=\frac{6\sum_{i=1}^{n}x_i m_i}{\pi\rho_s}\left[\frac{3\zeta_1\zeta_2-\zeta_2^3/\zeta_3^2}{1-\zeta_3}+\frac{\zeta_2^3/\zeta_3^2}{(1-\zeta_3)^2}+\frac{\zeta_2^3}{\zeta_3^2}\ln(1-\zeta_3)\right]-\sum_{i=1}^{k}x_i m_i\ln(1-\zeta_3) \qquad (4)$$

where

$$\zeta_l=\frac{\pi}{6}\rho_n\sum_{i=1}^{n}x_i m_i d_{ii}^{l} \quad (l=0,\ 1,\ 2,\ 3) \qquad (5)$$

$$\rho_s=\rho_n\sum_{i=1}^{n}x_i m_i \qquad (6)$$

In the above equations, ρ_n is the total number density of molecules in the solution, and d_{ii} is the hard-sphere diameter of segment i. Its relationship with the soft-sphere diameter (σ_{ii}) is based on the Barker-Henderson perturbation theory and is expressed by Cotterman (Cotterman et al. 1986) as follows

$$\frac{d_{ii}}{\sigma_{ii}}=\frac{1+0.2977kT/\varepsilon_{ii}}{1+0.33163kT/\varepsilon_{ii}+0.001047(kT/\varepsilon_{ii})^2} \qquad (7)$$

where ε_{ii} is the energy parameter of the L-J potential.

6.2.2. Hard Chain Formation Term

The chain term A^{chain} was derived by Chapman (Chapman et al. 1989)

$$\frac{A^{chain}}{NkT}=\sum_{i=1}^{n}x_i(1-m_i)\ln\left(g_{ii}^{hs}(d_{ii})\right) \qquad (8)$$

where

$$g_{ij}^{seg}(d_{ij})\approx g_{ij}^{hs}(d_{ij})=\frac{1}{1-\zeta_3}+\frac{3d_{ii}d_{jj}}{d_{ii}+d_{jj}}\frac{\zeta_2}{(1-\zeta_3)^2}+2\left[\frac{d_{ii}d_{jj}}{d_{ii}+d_{jj}}\right]^2\frac{\zeta_2^2}{(1-\zeta_3)^3} \qquad (9)$$

Eq.(9) for like segments becomes

$$g_{ii}^{hs}(d_{ii})=\frac{1}{1-\zeta_3}+\frac{3d_{ii}\zeta_2}{2(1-\zeta_3)^2}+\frac{d_{ii}^2\zeta_2^2}{2(1-\zeta_3)^3} \qquad (10)$$

6.2.3. Dispersion Term

This term is calculated by using an expression based on the Lennard-Jones potential (Cotterman et al. 1986)

$$\frac{A^{dis}}{NkT} = \sum_{i=1}^{n} x_i m_i \frac{1}{T_R}\left(A_1^{dis} + A_2^{dis}/T_R\right) \tag{11}$$

where

$$A_1^{dis} = \rho_R\left(-8.5959 - 4.5424\rho_R - 2.1268\rho_R^2 + 10.285\rho_R^3\right) \tag{12}$$

$$A_2^{dis} = \rho_R\left(-1.9075 + 9.9724\rho_R - 22.216\rho_R^2 + 15.904\rho_R^3\right) \tag{13}$$

$$T_R = kT/\varepsilon_x \tag{14}$$

$$\rho_R = \frac{6}{\sqrt{2}\pi}\zeta_3 \tag{15}$$

$$\varepsilon_x\sigma_x^3 = \sum_{i=1}^{n}\sum_{j=1}^{n} y_i y_j \varepsilon_{ij}\sigma_{ij}^3 \tag{16}$$

$$\sigma_x^3 = \sum_{i=1}^{n}\sum_{j=1}^{n} y_i y_j \sigma_{ij}^3 \tag{17}$$

$$y_i = \frac{x_i m_i}{\sum_{j=1}^{k} x_j m_j} \tag{18}$$

In the above equations, σ_{ij} and ε_{ij} are the cross parameters between different segments and are calculated by the following combining rules

$$\sigma_{ij} = \left(\sigma_{ii} + \sigma_{jj}\right)/2 \tag{19}$$

$$\varepsilon_{ij} = (1 - k_{ij})\sqrt{\varepsilon_{ii}\varepsilon_{jj}} \tag{20}$$

where k_{ij} is binary interaction parameter.

6.2.4 Association term

The Helmhotz energy due to association is calculated by the expression of Chapman (Champman et al. 1990)

$$\frac{A^{assoc}}{NkT} = \sum_i x_i \left[\sum_{A_i}\left(\ln X^{A_i} - X^{A_i}/2\right) + \frac{1}{2}M_i\right] \tag{21}$$

where M_i is number of associating sites on molecule *i*. The term X^{A_i} is defined as the mole fraction of molecules *i* not bonded at site A, in mixtures with other components, and is given by:

$$X^{A_i} = \left[1 + N_A \sum_j \sum_{B_j} x_j \rho X^{B_j} \Delta^{A_i B_j}\right]^{-1} \tag{22}$$

where $\sum_{B_j}$ means summation over all sites on molecule j, A_j, B_j, C_j, $\cdots$, $\sum_j$ means summation over all components, ρ is the total molar density of molecules in the solution, and $\Delta^{A_i B_j}$ is associating strength and is given by:

$$\Delta^{A_i B_j} = d_{ij}^3 g_{ij}(d_{ij})^{seg} \kappa^{A_i B_j} [\exp(\varepsilon^{A_i B_j} / kT) - 1] \tag{23}$$

In Eq.(23), κ^{AB} is the bonding volume and ε^{AB}/k as the associating energy. For cross-associating mixtures, we have the mixing rules

$$\kappa^{A_j B_i} = \kappa^{A_i B_j} = (\kappa^{A_i B_i} + \kappa^{A_j B_j})/2 \tag{24}$$

$$\varepsilon^{A_j B_i} = \varepsilon^{A_i B_j} = (1 - k_{ij}^{AB})\sqrt{(\varepsilon^{A_i B_i} \varepsilon^{A_j B_j})} \tag{25}$$

where k_{ij}^{AB} is binary associating interaction parameter.

6.3. Model for hydrate Phases

The introduction of inhibitor (alcohol) in a liquid water-hydrocarbon mixture alters the prevailing structure in the aqueous phase. Alcohol-water and alcohol-hydrocarbon molecular interactions result in a "less structured" organization of water molecules, thus reducing the possibility of forming stable hydrate. It is noted, however, that alcohol is not incorporated in the hydrate lattice (Davidson et al. 1977). Hence, the model of van der Waals and Platteeuw (van der Waals and Platteeuw, 1959), based on statistical mechanics, is valid and used in the work for the fugacity of water in the hydrate phase. It is expressed as follows:

$$f_W^H = f_W^{MT} \exp\left(\frac{-\Delta\mu_W^{MT-H}}{RT}\right) \tag{26}$$

where

$$\frac{-\Delta\mu_W^{MT-H}}{RT} = \sum_{m=1}^{2} (\nu_m \ln(1 + \sum_{j=1}^{n_c} C_{mj} f_j)) \tag{27}$$

here $\Delta\mu_W^{MT-H} = \mu_W^{MT} - \mu_W^H$, and it represents the difference between the chemical potential of water in the empty lattice (MT) and that in the hydrate lattice (H). C_{mj} is the Langmuir

constants and presents the gas-water interactions. It is given by John and Holder (John and Holder, 1982)-check:

$$C_{mj} = \frac{4\pi}{KT}\int_0^{R_m} \exp\left(\frac{-W_{mj}(r)}{KT}\right) r^2 dr \qquad (28)$$

here $W_{mj}(r)$ is the function for the cell potential, obtained from Mckoy and Sinanoglu (Mckoy and Sinanoglu, 1963).For temperatures above 260 K, the Langmuir constants are obtained from the expression of Parrish and Prausnitz (Parrish and Prausnitz, 1972)

The fugacity of water in the empty hydrate lattice, f_W^{MT} is obtained from the difference in the chemical potential of water in the empty lattice and that of pure liquid water, $\Delta\mu_W^{MT-L^o} = \mu_W^{MT} - \mu_W^{L^o}$, using the following equation (Holder et al. 1980):

$$f_W^{MT} = f_W^{L^o} \exp\left(\frac{-\Delta\mu_W^{MT-L^o}}{RT}\right) \qquad (29)$$

where $f_W^{L^o}$ is the fugacity of pure water, and it can be calculated from the SAFT equation state. The calculation of $\Delta\mu_W^{MT-L^o}$ is given elsewhere (Holder et al. 1980)

6.4. Parameters for SAFT

The SAFT equation requires three pure-component parameters for non-associating fluids and five parameters for associating fluids. These parameters are the L-J potential well depth (ε/k), the soft sphere diameter of segments (σ), the number of segments of the molecule (m), the bonding volume (κ^{AB}) and the association energy between sites A and B (ε^{AB}). In the case of mixtures, the SAFT equation uses van der Waals one-fluid mixing rules with the binary interaction parameter, k_{ij}, for the dispersion interactions and the parameter, k_{ij}^{AB}, for the associating interactions. In this work, these parameters required in the SAFT are taken from Li and Englezos and are shown in Table 17 and 18. As described in that work the four-site model are used for the hydrogen bonds of the water molecule and the two-site model for the hydrogen bonds of each hydroxyl group on the alcohol. It is noted that the binary interaction parameter, k_{ij} for the systems with EG, TEG or glycerol was taken equal to 0 since it was adequate to give satisfactory results

Table 17: Segment Parameters for Pure Fluids for the SAFT equation

Fluid	m	σ (10^{-10} m)	ε/k (k)	ε^{AB}/k (K)	κ^{AB}
Water	0.982	2.985	433.91	1195.20	0.038
Methanol	1.124	3.642	309.90	2320.77	0.019
EG	1.043	4.232	354.65	2375.26	0.020
Glycerol	2.180	4.194	405.08	2195.15	0.004
TEG	3.204	3.805	252.03	2470.02	0.061
Methane	1.186	2.990	160.84		
Ethane	1.437	3.193	199.73		
Propane	2.367	3.078	174.07		
CO_2	1.833	2.654	165.80		

Table 18: Binary Interaction Parameters for the SAFT equation

Systems	k_{ij}	Systems	k_{ij}
Methane/water	0.0291	Ethane/methanol	0.0641
Ethane/water	0.0068	CO_2/methanol	0.2025
CO_2/water	-0.0452	Methane/methanol	0.2204
Methanol/water	-0.1043		

6.5. Hydrate Formation Prediction

With the binary interaction parameters of the constituent binary subsystems and the molecular parameters of the pure components from Li and Englezos, the SAFT incorporated with the model of van der Waals and Platteeuw is employed to predict the hydrate formation conditions for the following nine systems: methane/water/methanol, ethane/water/methanol, CO_2/water/methanol, methane/water/glycerol, CO_2/water/glycerol, methane/water/ethylene glycol (EG), methane/water/triethylene glycol (TEG), ethane/water/triethylene glycol, propane/water/triethylene glycol. The incipient equilibrium hydrate formation pressure was calculated at a given temperature and at a given overall concentration of the inhibitor (methanol, EG, TEG and glycerol). The inhibitor concentration is usually reported as the water phase concentration possibly because when an experiment is conducted water is mixed with an amount of the inhibitor and the resulting concentration is reported. That concentration is considered the

overallconcentation in our calculation. It is noted that the overall concentrations must be specified in the isothermal isobaric flash calculation procedure. Table 19 summarizes the results. The absolute average deviation of predicted pressure (AAD (P), %) is defined as follows:

$$AAD(P)(\%) = \left(\frac{1}{N_P}\right)\sum_{i=1}^{N_P}\left[\left|\frac{T_{cal} - T_{\exp}}{T_{\exp}}\right|\right]_i \times 100$$

where N_P is the number of data points.

6.51. Inhibiting effect of Methanol

The experimental data along with predictions are given in figure 23, 24, 25 for methane, ethane and carbon dioxide hydrate. Table 19 also provides information about the AAD(P)%. As seen reasonably good predictions are obtained even at high pressures and at high methanol concentrations, it should be noted that the parameters required by the van der Waals model also play a role in the quality of the predictions.

Table 19 Predictions of the hydrate formation pressures

Gas	Concentration of inhibitor in aqueous phasse (wt%)	T-range (K)	P-range (MPa)	AAD (P) (%)			Data source
				This work	Sloan (1998)	Englezos et al.(1991)	
Methane	10% Methanol	266.2-286.4	2.14-18.8	1.87	3.48	3.31	(Ng and Robinson, 1985; Robinson and Ng, 1986)
	20% Methanol	263.3-280.2	2.83-18.75	4.36	1.26	7.37	
	35% Methanol	250.9-267.8	2.38-13.68	11.46	7.24	22.12	
	50% Methanol	233.1-255.3	1.47-16.98	18.53	9.95	53.62	
	10% EG	270.2-287.1	2.42-15.6	0.93			(Robinson and Ng, 1986)
	30% EG	267.6-280.1	3.77-16.14	0.59			
	50% EG	263.4-266.5	9.89-15.24	0.50			
	10% TEG	274.6-293	3.17-25.57	0.78			(Ross and Toczylkin, 1992)
	20% TEG	275-293	4.37-39.87	0.71			
	40% TEG	274.5-283	7.27-35.17	0.82			
	20% glycerol	273.8-286.2	4.39-20.53	0.36			(Ng and Robinson, 1994)
	50% glycerol	264.2-276.2	4.53-20.53	15.19			
Ethane	10% Methanol	268.3-281.4	0.417-2.8	0.63	3.27	10.21	(Ng and Robinson, 1985, Ng et al. 1985a, 1985b)
	20% Methanol	263.5-274.1	0.55-2.06	0.28	6.77	2.73	
	35% Methanol	252.6-262.2	0.502-1.48	0.29	14.06	11.35	
	50% Methanol	237.5-249.8	0.423-1.007	0.48	-	60.09	
	10% TEG	277-282	1.0-1.8	1.14			(Ross and Toczylkin, 1992)
	20% TEG	273.7-283	0.79-2.63	1.68			
	40% TEG	275-275.8	1.97-2.3	4.64			
Propane	10% TEG	272.3-276.8	0.18-0.51	1.69			(Servio and Englezos, 1997)
	20% TEG	271.7-275.2	0.25-0.50	1.88			
	30% TEG	270.2-272.4	0.29-0.425	0.31			
Carbon dioxide	10% Methanol	269.6-274.9	1.58-3.48	0.80	6.27	21.17	(Ng and Robinson, 1985; Robinson and Ng,1986)
	20% Methanol	264.0-268.9	1.83-2.94	2.11	15.15	26.37	
	35% Methanol	242.0-255.1	0.379-1.77	1.87	21.85	37.56	
	50% Methanol	232.6-241.3	0.496-1.31	0.69	-	57.21	
	10% glycerol	272.3-279.3	1.391-3.345	0.35			(Ng and Robinson, 1994; Breland and Englezos, 1996)
	20% glycerol	270.4-277.1	1.502-3.556	2.32			
	25% glycerol	269.6-276.8	1.48-3.96	0.43			
	30% glycerol	270.1-273.2	2.03-2.981	2.74			

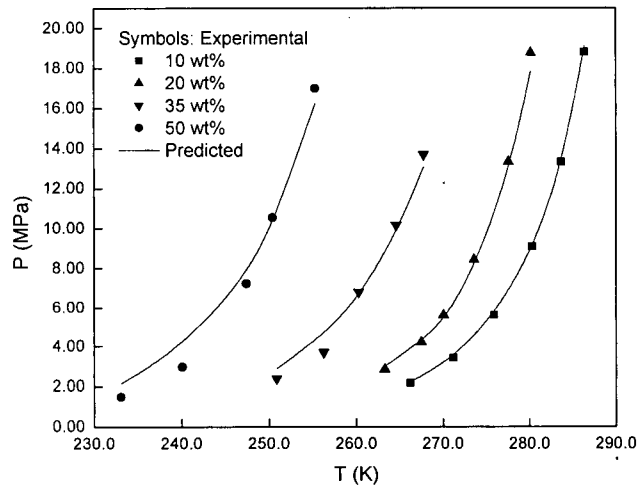

Figure 23: Methane hydrate formation in the presence of methanol: data and predictions based on SAFT

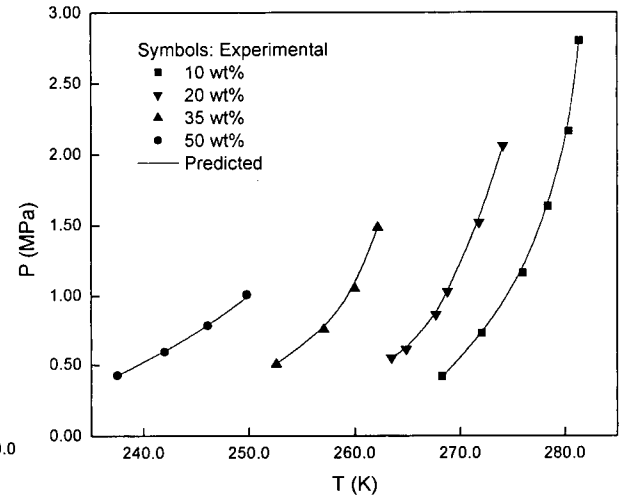

Figure 24: Ethane hydrate formation in the presence of methanol: data and predictions based on SAFT

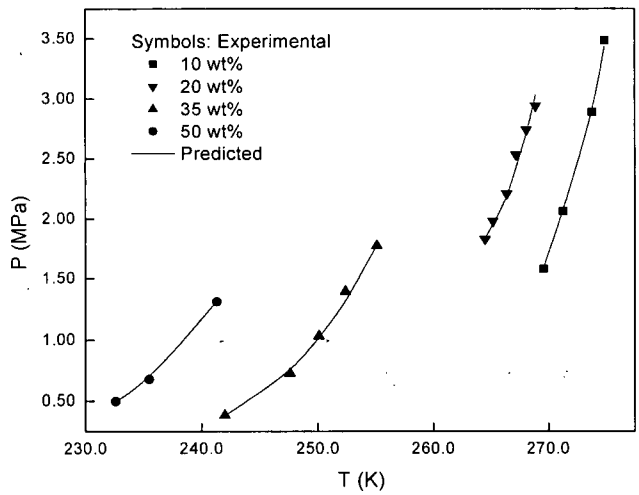

Figure 25: CO_2 hydrate formation in the presence of methanol: data and predictions based on SAFT

6.5.2. Inhibiting effect of Ethylene Glycol

Table 19 and Figure 26 present the prediction of inhibiting effect of ethylene glycol (EG) on methane hydrate formation with 10-50% of EG using the SAFT equation. As seen, the predictions compare quite well with the experimental data. The total AAD is 0.67%. The maximum deviation is only 0.93%. This demonstrates the excellent prediction function of the SAFT. EG molecule has more functional groups for association than methanol. Thus its

associating behavior is expected to be stronger than that of methanol. It can be seen from the above calculations that the stronger the associating behavior of the fluid is, the stronger the prediction ability of the Molecular-based SAFT.

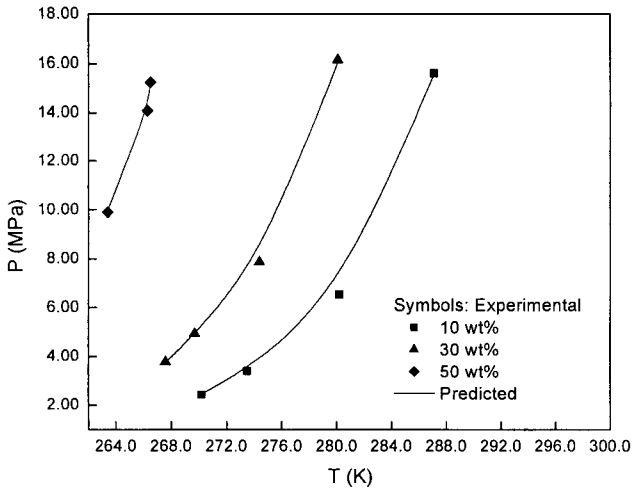

Figure 26: Methane hydrate formation in the presence of ethylene glycol: data and predictions based on SAFT

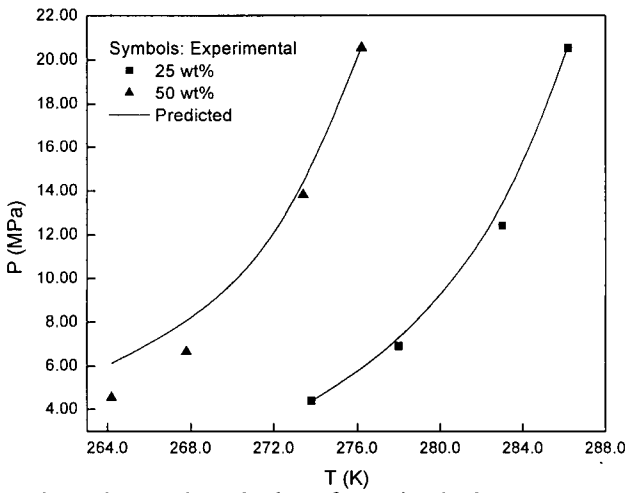

Figure 27: Methane hydrate formation in the presence of glycerol: data and predictions based on SAFT

6.5.3. Inhibiting effect of Glycerol

The SAFT equation was also employed to predict the inhibiting effect of glycerol on the hydrate formation of methane and CO_2, respectively. The results are presented in Table 19 and Figures 27 and 28. As seen, the prediction on methane hydrate formation is excellent and the deviation is only 0.36% at 25% of glycerol. At 50% of glycerol, a deviation of 15.19% is acceptable. Finally the calculated pressures for the CO_2/glycerol/ water system with SAFT are in quite good agreement with the data at low and high concentrations of glycerol. The total AAD is 1.46%.

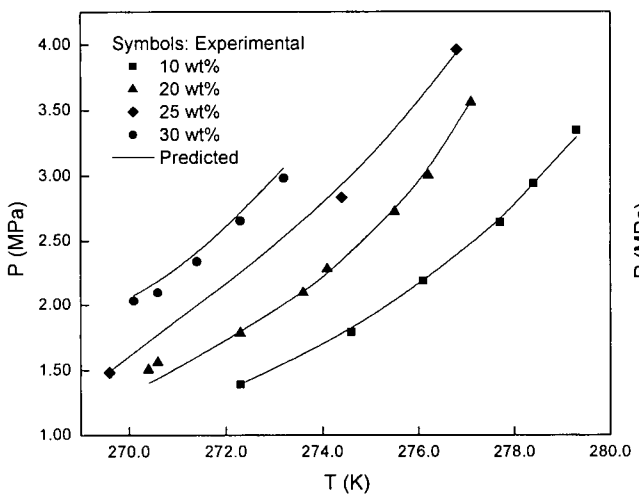

Figure 28: CO_2 hydrate formation in the presence of glycerol: data and predictions based on SAFT

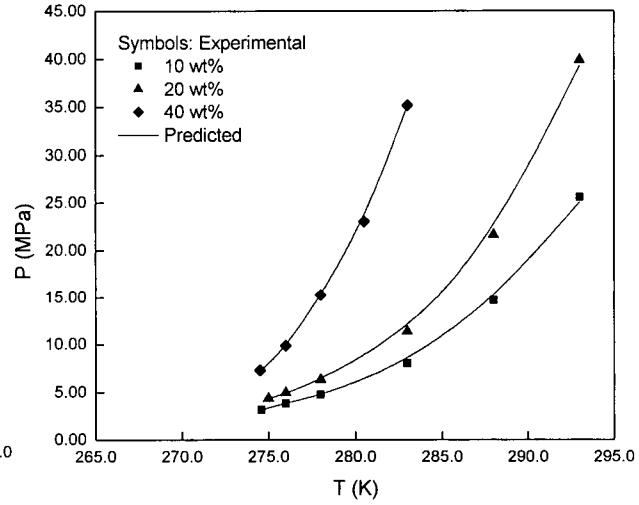

Figure 29: Methane hydrate formation in the presence of TEG: data and predictions based on SAF

6.5.4 Inhibiting effect of Triethylene Glycol

The inhibiting effect of TEG on the hydrate formation from methane, ethane and propane, was also computed using SAFT. The results are shown in Table 19 and Figures 29-31. The total predicted ADDs are 0.77%, 2.49% and 1.29% for the methane/TEG/water, ethane/TEG/water and propane/TEG/water, respectively. The agreement between predictions and data is quite good.

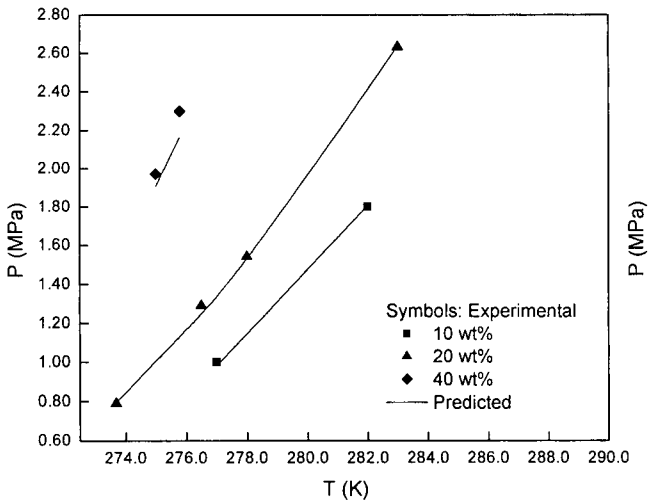

Figure 30: Ethane hydrate formation in the presence of TEG: data and predictions based on SAFT

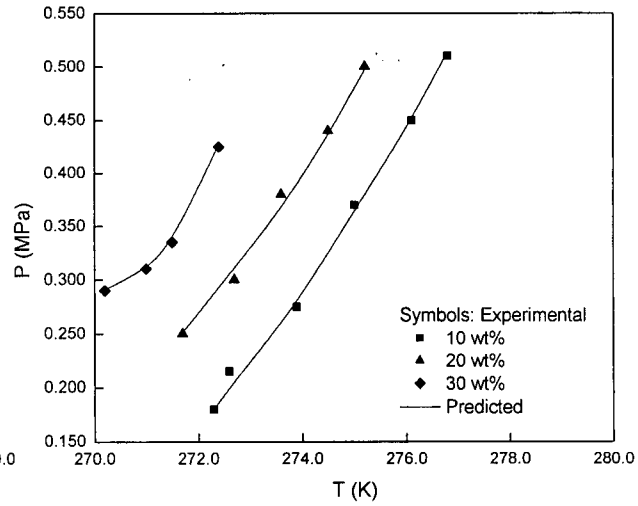

Figure 31: Propane hydrate formation in the presence of TEG: data and predictions based on SAFT

6.5.5. Discussion

As seen from the above calculations SAFT results in satisfactory to excellent predictions of the inhibiting effect of methanol, EG, glycerol and TEG on gas hydrate formation. The SAFT models takes into account chain formation and molecular associating interactions in addition to repulsion and dispersion. In systems containing inhibitors (methanol, EG, glycerol and TEG) and water association interactions are expected to be strong. Accordingly, the association term in the SAFT model is significant and plays a very important role for the prediction of gas hydrate formation in the presence of the inhibitors.

7. Conclusion and Recommendations

7.1. Conclusion

Triethylene glycol (TEG) and glycerol are common thermodynamic inhibitors used in the gas and oil industries. Knowing their inhibiting abilities is very important not only for in-situ guidelines but also valuable for validating the hydrate prediction models. In this work, inhibiting effects of TEG and glycerol were determined experimentally through incipient hydrate formation measurements using a 91-9 mol % mixture of methane and ethane and a 90.5-9.5 mol % mixture of methane and propane. The concentrations of the TEG in the water phase werr 20 and 30 wt % whereas that of glycerol was 20 wt %. Moreover the inhibiting effects were also calculated by using the van der Waals Platteeuw model for the hydrate and two equations of state for the fluid phases (Trebble-Bishnoi equation of state and SAFT). The SAFT model was employed for the prediction of the thermodynamic inhibiting on single gas hydrate formation only. Both models performed reasonably well for engineering-type calculations.

7.2. Recommendations

First, the use of a direct cooling system is recommended in order to minimize temperature fluctuations. Second, it is recommend flushing the sampling tube with Helium since more than the pressure dropped by more than 3 psi after taking gas sample at equilibrium condition using gas sampling tube. Finally, the computational methodology using the SAFT model should be extended to deal with hydrate formation from gas mixtures too.

8. References

Anderson, F. E.; Prausnitz, J. M. Inhibition of Gas Hydrates by Methanol. *AIChE J.* **1986**, 32, 1321-1333.

Avlonitis, D; Todd, A. C.; Danesh, A. A Rigorous Method for the Prediction of Gas Hydrate Inhibition by Methanol in Multicompont Systems. Proc. First Int. Offshore and Polar Engineering Conf., Edinburgh, 11-16 August **1991**, Int. Soc. Of Offshore and Polar Engineers.

Berecz, E.; Balla-Achs, M. Study in Inorganic Chemistry 4: Gas hydrates; Elsevier: Amsterdam, **1983**; 184-188.

Bishnoi, P.R.; Pankaj D; Dholabhai, J. Equilibrium Conditions for Hydrate Formation for a Ternary Mixture of Methane, Propane and Carbon Dioxide, and a Natural Gas Mixture in the Presence of Electrolytes and Methanol. *Fluid Phase Equilibria* 158-160 (**1999**) 821-827.

Boublik, T. *J. Chem. Phys.* **1970**, 53, 471.

Breland, Ed.; Englezos, P. J. *Chem. Eng. Data.* **1996**, 41, 11-13.

Cartaya, E.; Harmon, S.; Starling, K.E. Evaluation of the local composition model for VLE of binary mixture of tri-ethylene glycerol with methane, water and benzene. *Fluid Phase Equilibria* **1996**, 74, 411-418.

Chapman, W.G.; Gubbins, K.E.; Jackson, G.; Radosz , M. *Ind. Eng. Chem. Res.* **1990**, 29, 1709.

Chapman,W.G.; Gubbins, K. E.; Jackson , G.; Radosz, M. *Fluid Phase Equilib.* **1989**, 52, 31.

Cotterman RL, Schwarz BJ, Prausnitz JM. Molecular thermodynamics for fluids at low and high densities. Part 1: Pure fluids containing small or large molecules. AIChE J. **1986**;32(11):1787-1798.

Davidson, D.W.; Garg, S.K.; Gough, S.R.; Haqkings, R.E.; Ripmeester, J.A. Characterization of Natural Gas Hydrates by Nuclear Magnetic Resonance and Dielectric Relaxation; *Can. J. Chem.* **1977**, 55, 3641-3650.

Davidson, D.W., gas hydrates. In: Frank F, Eds., Water: a comprehensive treatise, Plenum Press, New York, **1973**, 2(3), 115-234

Dholabhai, P.D.; Englezos, P.; Kalogerakis, N.E.; Bishnoi, P.R. Equilibrium Condition for Methane Hydrate Formation in Aqueous Mixed Electrolyte Solutions. *Can. J. Chem. Eng.* **1991a**, 69, 800-805.

Dholabhai, P.D.; Parent, J.S.; Bishnoi, P.R. Carbon Dioxide Hydrate Equilibrium Conditions in

Aqueous Solutions Containing Electrolytes and Methanol Using a New Apparatus, *Ind. Eng. Chem. Res.* **1996**, 35, 819-823.

Eichholz, C.; Majumdar, A.; Clarke, M.A.; Oellrich, L.R.; Bishnoi, P.R. Experimental Investigation and Calculation of Methane Hydrate Formation Conditions in the Presence of Ethylene Glycol and Sodium Chloride. *J. Chem. Eng. Data* **2004**, 49, 847-851.

Englezons, P.; Huang, Z.; Bishnoi, P.R. Prediction of Natural Gas Hydrate Formation Conditions in the Presence of Methanol Using the Trebble-Bishnoi Equation of State. *The Journal of Canadian Petroleum Technology*. **1991**, 30, 148-155.

Englezos, P. Clathrate Hydrate. *Ind. Eng. Chem. Res.* **1993**, 32, 1251-1274.

Englezos, P.; Bishnoi, P. R. Experimental Study on the Equilibrium Ethane Hydrae Formation Conditions in Aqueous Electrolyte Solutions. *Ind. Eng. Chem. Res.* **1991**, 30, 1665-1659.

Englezos, P.; Ngan, Y.T. Effect of Polyethylene Oxide on Gas Hydrate Phase Equilibra. *Fluid Phase Equilib.* **1994**, 92, 271-288.

Englezos, P.; Ngan, Y.T. Incipient Equilibrium Data for Propane Hydrae Formation in Aqueous Solutions of NaCl, KCl and $CaCl_2$. *J. Chem. Eng. Date* **1993a** ,38, 250-253

Hammerschmidt, E.G. Formation of Gas Hydrates in Natural Gas Transmission Lines. *Ind. Eng. Chem.* **1934**, 26, 851-855.

Holder, G.D.; Gorbin, G.; Papadopoulos, K.D. Thermodynamic and Molecular Properties of Gas Hydrate from Mixtures Containing Methane, Argon, and Krypton, *Ind. Eng. Chem. Fundam.* **1980**, 19, 282-286.

John, V.T.; Holder, G.D. Contribution of Second and Subsequent Water Shells to the Potential Energy of Guest-Host interactions in Clathrate Hydrates; *J. Chem. Phys.*, **1982**, 96, 455-459.

Katz, D.L. Depths to Which Frozen Gas Fields (Gas Hydrate) may be expected. *J.Pet. Tehnol.* **1971**, 419-423.

Jou, F.Y.; Deshmukh, R.D.; Otto, A.D., mather, A.E. Vapor liquid equilibria for acid gases and lower alkanes in triethylene glycerol. *Fluid phase equilibria,* **1987**, 36, 121-140

Kvenvolden, K.A. Methane Hydrate-A major Reservoir of Carbon in the Shallow Geosphere. *Chemical Geology* **1988**, 71 (1-3), 41-51.

Li, X.-S.; Englezos, P. Vapor-Liquid Equilibrium of Systems Containing Alcohols Using the Statistical Associating Fluid Theory Equation of State. *Ind. Eng. Chem. Res.* **2003**, 42, 4953-4961.

Li, X.-S.; Englezos, P. Vapor-Liquid Equilibrium of Systems Containing Alcohols, Water, Carbon Dioxide and Hydrocarbons Using SAFT. *Fluid Phase Equilib.* **2004**, 224, 111-118.

Mahmodaghdam, E; Bishnoi, P.R. Equilibrium Data for Methane, Ethane, and Propane Incipient Hydrate Formation in Aqueous Solutions of Ethylene Glycol and Diethylene Glycol. *J. Chem. Eng. Data* **2002**, 47, 278-281

Makogon, Y. F. Hydrates of Natural Gas; Penn Well Publishing; Tulsa, OK, **1981**.

Makogon, Y.F.; Trebin, F.A.; Trofimuk, A.A.; Tsarev, V.P.; Chersky, N.V.Detection of a Pool of Natural Gas in a Solid (hydrate gas) State. Dokl. Acad. Sci. USSR-Earth Sci. Sect. **1972**, 196, 197-200.

Mansoori, G. A.; Carnahan, N. F.; Starling , K.E.; Leland, T. W. *J. Chem. Phys.* **1971**, 54, 1523.

Mckoy , V.; Sinanoglu, O. Theory of Dissociation Pressures in Some Gas Hydrates. *J. Chem. Phys.* **1963,** 38, 2946-2956.

Muller, E. A.; Gubbins, K. E. *Ind. Eng. Chem. Res.*, **2001**, 40, 2193-2211.

Ng, H.-J.; Robinson, D.B. Hydrate Formation in Systems Containing Methane, Ethane, Propane, Carbon Dioxide or Hydrogen Sulfide in the Presence of Methanol. *Fluid Phase Equilib.* 1**985,** 21, 145-155.

Ng., H.-J.; Chen, C.-J.; Robinson, D. B. Gas Proc. Assn. Rsch. Rpt. **1985a**, 87, March.

Ng., H.-J.; Chen, C.-J.; Robinson, D. B. Gas Proc. Assn. Rsch. Rpt. **1985b**, 92, September.

Ng., H.-J.; Robinson, D. B. (First) International Conference on Natural Gas Hydrates, Annals of New York Academy of Sciences. **1994**, 715, 450.

Pankaj D; Dholabhai, J; Scott Parent ; Bishnoi, P.R.. Equilibrium Conditions for Hydrate Formation from Binary Mixtures of Methane and Carbon Dioxide in the Presence of Electrolytes, Methanol and Ethylene Glycol. *Fluid Phase Equilibria* **1997**,14, 235-246.

Parrish, W.R.; Prausnitz, J.M. Dissociation Pressures of Gas Hydrate Formed by Gas Mixtures. *Ind, Eng. Chem. Process Desigh Develop.* **1972**, 11, 26-34.

Pfohl, O.; Pagel, A.; Brunner, G. *Fluid Phase Equilib.* **1999**, 157, 53.

Ripmeester, J.A.; Tse, J.S.; Ratcliffe, C.I. and Powell, B.M. A new clathrate hydrate structure, *Nature.* **1987**, 325, 135-136

Ripmeester, J.A.; Ratcliffe, C.I. Xenon-129 NMR studies of clathrate hydrates: new guests for structure II and structure H, *Journal of Physical Chemistry.* **1990**, 94(25), 8773-8776.

Ripmeester, J.A.; Ratcliffe, C.I.; Klug, D.D., Tse, J.S. Molecular perspectives on structure and dynamics in clathrate hydrates, Annals of the New York Academy of Sciences 715 (International conference on natural gas hydrates, 1993). **1994**, 161-176.

Robinson, D.B.; NG, H.-J. Hydrate Formation and Inhibition in Gas or Gas Condensate Streams. *Journal of Canadian Petroleum Technology*. **1986**, 25, 26-30.

Roch, Armin. Experimental and Theoretical Studies of Hydrate Formation of as Mixtures in Inhibitor-containing Aqueous Solutions. Fortschritt-Berichte VDI, Reihe 3: Verfahrenstechnik **2003,** 768 i-xiii, 1-279.

Ross, M. J.; Toczylkin, L. S. J. *Chem. Eng. Data*. **1992**, 37, 488.

Ross, M.J; Toczylkin, L.S. Hydrate Dissociation Pressures for Methane or Ethane in the Presence of Aqueous Solutions of Triethylene Glycol. *J. Chem, Eng. Date* **1992,** 37, 488-491

Servio, P; Englezos, P. Incipient Equilibrium Propane Hydrate Formation Conditions in Aqueous Triethylene Glycol Solution. *J. Chem. Eng. Data*. **1997**, 42, 800-801.

Servio, P; Englezos, P. Incipient Equilibrium Propane Hydrates Formation Conditions in Aqueous Triethylene Glycol Solution. *J. Chem. Eng. Data* **1997**, 42, 800-801

Servio, Phillip. Incipient Equilibrium Gas Hydrates Formation Conditions for the CO2-CH4-neohexane-NaCl-H2O and CH4-polypropylene glycol-NaCl-H2O Systems. *International journal of the Society of Materials Engineering for Resources*. **1999,** 7(1), 24-28.

Sloan, E. D. Cathrate Hydrates of Natural Gases. **1998**: Marcel Dekker, New York.

Song, K. Y.; Kobayashi, R. Final Hydrate Stability Conditions of a Methane and Propane Mixture in the Presence of Pure Water and Aqueous Solutions of Methanol and Ethylene Glycol. *Fluid Phase Equilib*. **1989**, 47, 295-308

Sloan, E. D. Jr. Clathrate Hydrates of Natural Gases, 2nd edition, Marcel Dekker, New York, **1990**.

Sloan, E. D. Jr. Clathrate Hydrates of Natural Gases, 1st edition, Marcel Dekker, New York, **1998.**

Svartas, T.M.; Fadnes, F.H. Methane Hydrate Equilibrium Date for the Methane-Water-Methanol System up to 500 bara. Proceedings, second (1992) International offshore and Polar Engineering Conference, San Francisco, June 14-19, **1992**; Chung, J.S.,Natvig, B.J. Li, Y-C., Das, B.M., Eds.;pp 614-619.

Trebble, M.A.; Bishnoi, P.R. Extension of the Trebble-Bishnoi equation of state to fluid mixtures *Fluid Phase Equilibria*.**1988,** 40, 1-21.

Voutsas, E. C.; Boulougouris G. C.; Economou, I. G.; Tassios, D. P. *Ind. Eng. Chem. Res.* **2000**, 39, 797-804.

Wertheim, M. S. J. *Chem. Phys.* **1986**, 87, 7323.

van der Waals, J.H. The statistical mechanics of clathrate compounds. *Trans. Faraday Soc.* **1956,** 52, 184-193.

van der Waals, J.H.; Platteeuw, J.C. Clathrate Solutions. *Adv. Chem. Phys.*, **1959**, 2, 1-57.

Appendix A: Pressure Calibration Curve

HEISE Digital Pressure Indictor-90 IA used in the experiment was calibrated using a pressure gauge (WIKA 27888DA) with accuracy of 50KPa. The calibration result is shown in Table A-1 and plotted in figure A-1.

Table A-1: original data for pressure calibration

	Pressure from HEISE Digital Pressure Indictor-90 IA (KPa)	Pressure from WIKA 27888DA (KPa)
Point 1	0.00	0.00
Point 2	1016	1014
Point 3	2058	2055
Point 4	2995	2992
Point 5	4047	4047
Point 6	4873	4875
Point 7	5900	5901
Point 8	6632	6633

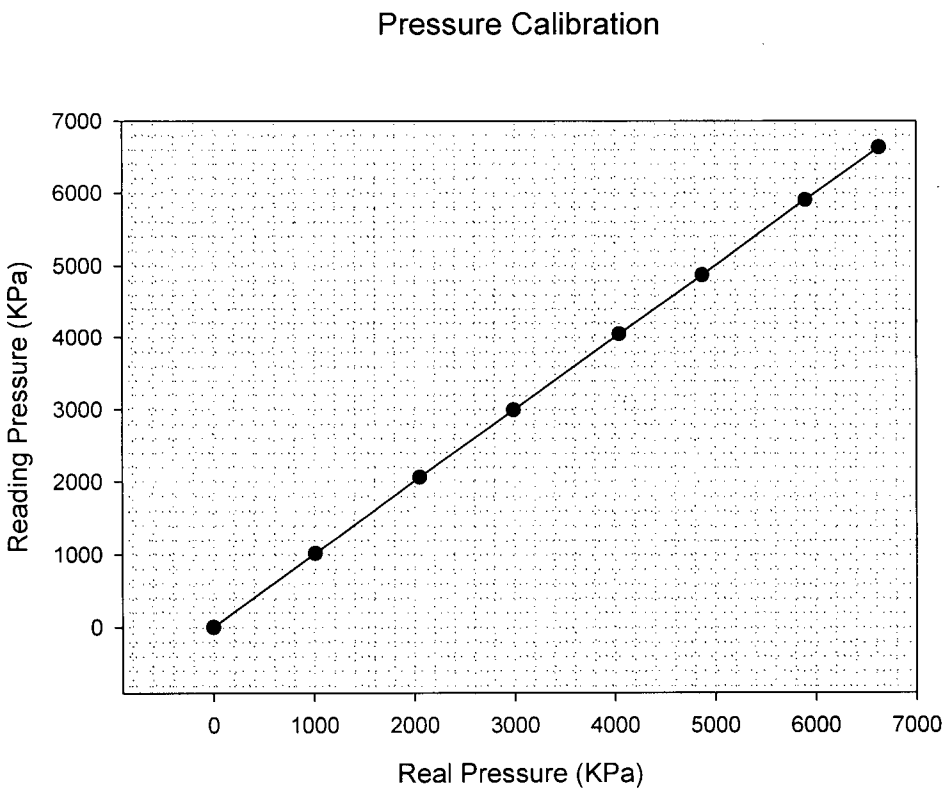

Appendix B: Thermocouple calibration Curve

The Copper-constant thermocouple (Omega, ±0.1°C accuracy) used in the experiment was calibrated using the standard thermometer .The calibration results are shown in the table B-1 and plotted in the figure B-1

Table B-1: original data for thermocouple calibration

	Temperature from standard thermometer (°C)	Temperature form the thermocouple (°C)
Point 1	5.33	5.9
Point 2	4.44	4.9
Point 3	3.44	3.8
Point 4	2.61	2.8
Point 5	1.50	1.7
Point 6	0.22	0.3
Point 7	-0.33	-0.2

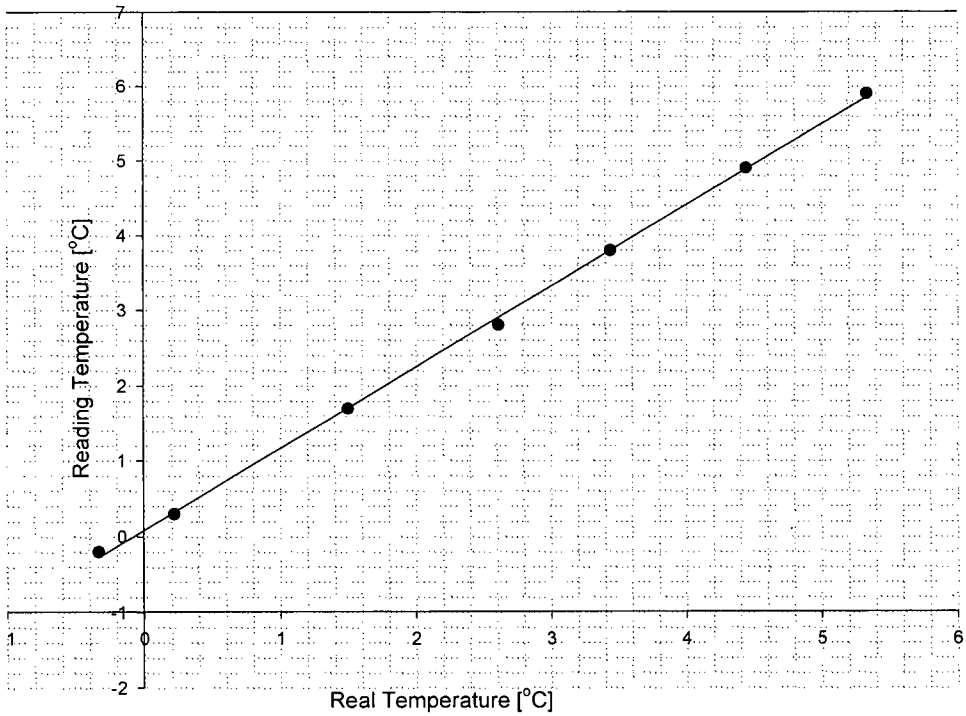

Figure B-1: thermocouple calibration curve

APPENDIX C: The sample of calibrating gas composition from gas cylinder

The gas composition from gas cylinder always changes with the time. Before starting the experiment, the gas composition from gas cylinder was calibrated based on analysis results of GC. The pure methane gas was used as standard gas. A sample of calibrating the gas composition from methane-ethane cylinder is shown in the bellow (the original gas composition from the cylinder is 90.0% of methane and 10.0% of ethane).

1. Injecting five gas samples of the pure methane and methane-ethane gas mixture from gas cylinders to GC separately. The results were shown in table C-1 and C-2.

Table C-1: Peak areas of pure methane and methane-ethane gas samples from cylinders

	Sample 1	Sample 2	Sample 3	Sample 4	Sample 5	**Average**
Peak area of pure methane	1674355	1681198	1663087	1668086	1676407	**1672627**
Peak area of methane in mixture	1522968	1529976	1511419	1524300	1519501	**1521633**

Table C-2: Peak area percentages of methane and ethane gas samples from gas cylinders.

	Sample 1	Sample 2	Sample 3	Sample 4	Sample 5	**Average**
Area % of methane in gas mixture	80.72	80.66	80.64	80.58	80.62	**80.64**
Area % of ethane in gas mixture	19.28	19.34	19.36	19.42	19.38	**19.36**

2. the real gas composition from methane-ethane gas cylinder can be calculated as follows:

Methane in mixture=peak area of pure methane/peak area of methane in mixture=1521633/1672627=90.97%

Ethane in mixture =100%-90.97%=9.03%

3. after calibrated the gas composition from the cylinder, response factor was also calculated as follows:

Considering the response factor of methane is equal to 1, and then the response factor of ethane is calculated as follows:

Response factor= (area percentage of ethane/real composition of ethane)/ (area percentage of mthane/real composition of methane)

= (19.36/9.03)/ (80.64/90.97)=2.419

Appendix D: The sample of calculating gas composition in hydrate equilibrium condition.

Three gas samples were taken to do GC analysis when hydrate was in equilibrium condition. The following shows how to calculate gas composition in hydrate equilibrium condition based on methane-ethane (9.03%)-TEG (20.2%)-H2O system at 276.5 K, and the related GC date are shown in the table C-1.

Table D-1: GC data for the on methane-ethane (9.03%)-TEG (20.2%)-H2O system at 276.5 K

	Peak percentage (%)		Composition (%)		sum	Concentration (%)	
	methane	ethane	methane	ethane		methane	ethane
Sample 1	81.382	18.618	81.382	7.698	89.080	91.36	8.64
Sample 2	81.531	18.469	81.531	7.636	89.167	91.44	8.56
Sample 3	81.275	18.725	81.275	7.742	89.017	91.30	8.70
average						**91.37**	**8.63**

The peak percentages of three samples obtained from GC analysis are shown in the second and third columns. The gas composition of each sample which shown in third and forth columns is equal to the peak percentage divided by response factor. The sum of the composition of methane and ethane is given in the fifth column. Then the concentration of methane or ethane is equal to their composition divided by sum as shown in the last two columns. Finally the average gas composition is obtained as shown in the table.

Appendix E: original data for calibrating gas composition from C1-C3 gas cylinder

Table E-1: Peak areas of pure methane and methane-propane gas samples from cylinder

	Sample 1	Sample 2	Sample 3	Sample 4	Sample 5	**Average**
Peak area of pure methane	1674355	1681198	1663087	1668086	1676407	**1672627**
Peak area of methane in mixture	1500568	1490058	1545065	1512791	1527514	**1515199**

Table E-2: Peak area percentages of methane and propane gas samples from gas cylinder.

	Sample 1	Sample 2	Sample 3	Sample 4	Sample 5	**Average**
Area % of methane in gas mixture	76.24	76.24	76.22	76.19	76.20	**76.22**
Area % of ethane in gas mixture	23.76	23.76	23.78	23.81	23.80	**23.78**

Appendix F: original GC analysis data in hydrate equilibrium conditions for the C1-C2-TEG (20.2%) systems.

Table F-1: original GC analysis data in hydrate equilibrium conditions for the C1-C2-TEG (20.2%) systems.

		Area % of methane in gas mixture	Area % of ethane in gas mixture
Point 1@ 282.0K	Sample 1	81.62	18.38
	Sample 2	81.43	18.57
	Sample 3	81.51	18.49
Point 2 @ 280.8K	Sample 1	81.44	18.56
	Sample 2	81.36	18.64
Point 4 @276.5KK	Sample 1	81.38	18.62
	Sample 2	81.27	18.73
	Sample 3	81.27	18.73
Point 5 @274.9K	Sample 1	81.56	18.44
	Sample 2	81.55	18.45
	Sample 3	81.44	18.56
Point 6@272.6K	Sample 1	81.71	18.29
	Sample 2	81.53	18.47
	Sample 3	81.51	18.49

Table F-2. Original GC analysis data for the system with 30% TEG using the CP-3800 GC

		Area % of methane in gas mixture	Area % of ethane or in gas mixture
C1-C2-30%TEG	Point 1		
	Point 2@279.4K	80.86	19.14
	Point 3@277.4K	80.64	19.36
	Point 4@275.3K	80.91	19.09
	Point 5 @273.8K	80.95	19.05

Appendix G: original GC analysis data in hydrate equilibrium condition for the C1-C3-TEG (0%, 20.0%, and 30.0%) systems.

Table G-1. original GC analysis data for the system with 0% and 20% TEG using the CX-3400 GC.

			Area % of methane in gas mixture	Area % of propane in gas mixture
0%TEG	Point 3@ 277.0K	Sample 1	71.6	28.4
		Sample 2	71.21	28.79
	Point 4 @ 275.4	Sample 1	71.55	28.45
	Point 5 @273.6K	Sample 1	71.19	28.81
		Sample 2	72.21	28.79
20% TEG	Point 1 @281.4K	Sample 1	74.63	25.37
		Sample 2	73.69	26.31
		Sample 3	73.77	26.23
	Point 2 @279.5K	Sample 1	73.36	26.64
	Point 3 @277.3K	Sample 1	74.06	25.94
		Sample 2	73.92	26.08
	Point 4 @275.4K	Sample 1	72.27	27.73
		Sample 2	72.14	27.86
30.0%TEG	Point 1@281.7K	Sample 1	73.48	26.52
	Point 2@277.8K	Sample 1	73.01	26.99
	Point 3@276.0K	Sample 1	74.0	26.0

Appendix H: original GC analysis data in hydrate equilibrium condition for C1-C2-Glycerol (20.0%) and C1-C3-Glycerol (20.0%) systems.

Table H-1: original GC analysis data in hydrate equilibrium condition for C1-C2-Glycerol (20.0%) and C1-C3-Glycerol (20.0%) systems suing CP-3800 GC

		Area % of methane in gas mixture	Area % of ethane or propane in gas mixture
C1-C2-20%glycerol	Point 1@281.3K	80.71	19.29
	Point 2@280.1K		
	Point 3@278.8K	80.72	19.28
	Point 4@276.3K	81.28	18.72
	Point 5@274.2K	80.90	19.10
C1-C3-20%glycerol	Point 1@280.3K	73.16	26.84
	Point 2@278.3K	73.14	26.86
	Point 3@275.7K	72.15	27.25
	Point 4@274.2K	72.84	27.16

Appendix I: Calculation of hydrate point depression (ΔT_H)

The method of calculating the hydrate point depression is explained as follows based on the C1-C3-TEG (0%, 20.0%, and 30.0%) hydrate formation systems.

Firstly, the experimental data which is shown in the table I-1 is plotted on the figure I-1, and then quadratic equation ($y = y_0 + ax + bx^2$) is selected to fit the data and the fitting curves are shown on the figure I-1 as well. The hydrate point depression at each pressure point can be obtained roughly. For example, at 1000KPa, a horizontal line is drawn which crosses the three equilibrium curves, and then vertical lines are drawn from interactions, so the temperature can be obtained and is shown in the table I-2. The hydrate point depression at 1000KPa can be calculated and presented in the table I-2 as well.

Table I-1: experimental data for C1-C3-TEG (0%, 20.0%, and 30.0%) hydrate formation systems

Concentration of TEG (mass %)	Temperature/K	Temperature/^{0}C	Pressure/KPa
0	280.6	7.5	1190.4
	278.9	5.8	990.4
	277.0	3.9	783.4
	275.4	2.3	645.0
	273.6	0.5	521.6
20	281.4	8.3	1756.0
	279.5	6.4	1418.0
	277.3	4.2	1142.1
	275.4	2.3	915.0
	273.6	0.5	750.0
30	281.7	8.6	2211
	280.0	6.9	1831
	277.8	4.7	1390
	276.0	2.9	1120
	274.2	1.1	900

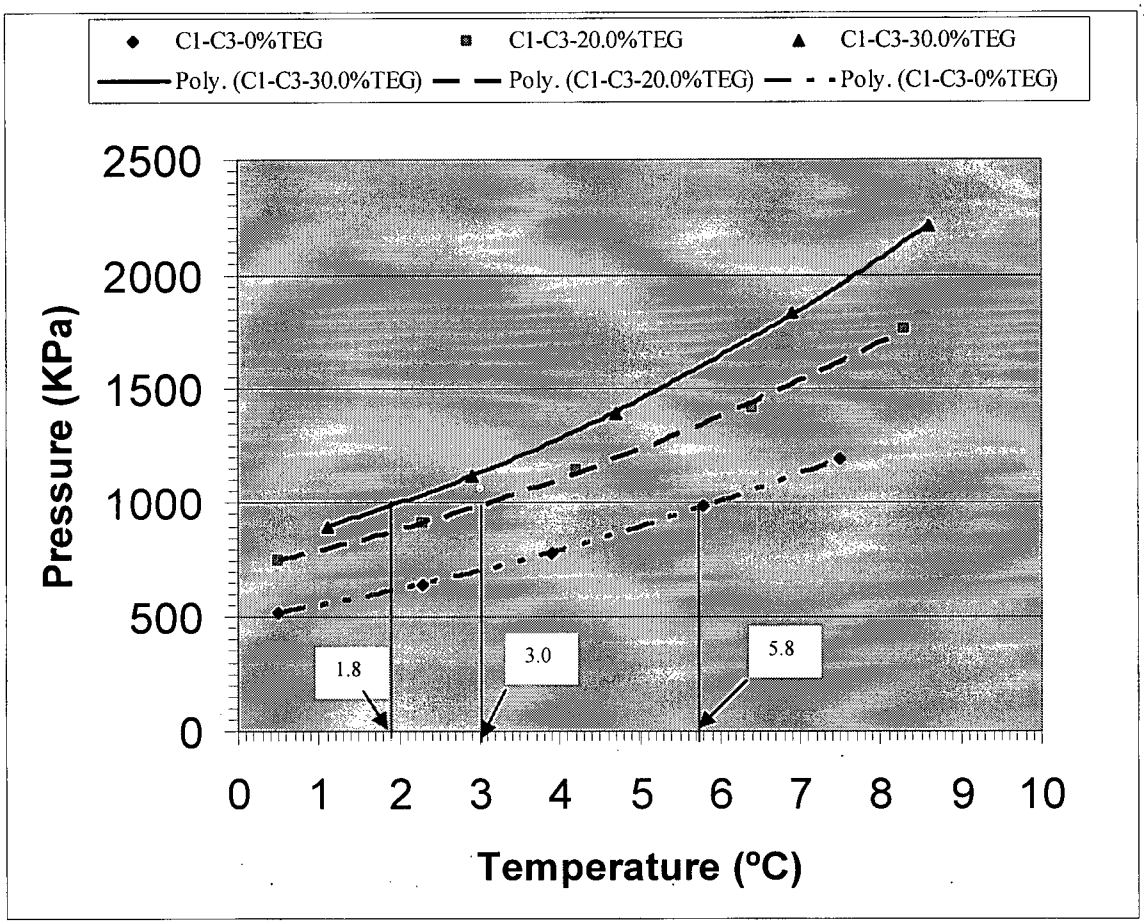

Figure I-1: experimental data and fitting curves

Table I-2: temperatures of three hydrate formation systems and Hydrate point depression (ΔT_H) at 1000MPa

	Temperature (^{0}C)	Hydrate point depression ΔT_H
C1-C3-0%TEG	5.8	0 (5.8-5.8)
C1-C3-20.0%TEG	3.0	2.0 (5.8-3.0)
C1-C3-30.0%TEG	1.8	4.0 (5.8-1.8)